

Supplemental Material

Salaverria et al

Contents

I.	Members of the network project of the Deutsche Krebshilfe “Molecular Mechanisms in Malignant Lymphomas”.....	Page 2
II.	Supplemental material and methods.....	Page 3
III.	Supplemental results and discussion.....	Page 11
IV.	Supplemental tables.....	Page 14
V.	Supplemental figures.....	Page 36
VI.	Supplemental references.....	Page 47

I. Members of the Network Project of the Deutsche Krebshilfe “Molecular Mechanisms in Malignant Lymphomas” (Alphabetical order)

Pathology group: Thomas F.E. Barth¹, Heinz-Wolfram Bernd², Sergio B. Cogliatti³, Alfred C. Feller², Martin L. Hansmann⁴, Michael Hummel⁵, Wolfram Klapper⁶, Peter Möller¹, Hans-Konrad Müller-Hermelink⁷, Ilske Oschlies⁶, German Ott²⁰, Andreas Rosenwald⁷, Harald Stein⁵, Monika Szczepanowski⁶, Hans-Heinrich Wacker⁶. **Genetics group:** Thomas F.E. Barth¹, Petra Behrmann⁸, Peter Daniel⁹, Judith Dierlamm⁸, Eugenia Haralambieva⁷, Jose-Ignacio Martín-Subero¹⁰, Paul-Martin Holterhus¹¹, Ralf Küppers¹², Dieter Kube¹³, Peter Lichter¹⁴, Peter Möller¹, Eva M. Murga-Peñas¹⁰, German Ott²⁰, Claudia Philipp¹², Christiane Pott¹⁵, Armin Pscherer¹⁴, Julia Richter¹⁰, Andreas Rosenwald⁷, Carsten Schwaenen¹⁶, Reiner Siebert¹⁰, Heiko Trautmann¹⁵, Martina Vockerodt¹⁷, Swen Wessendorf¹⁶. **Bioinformatics group:** Stefan Bentink¹⁸, Hilmar Berger¹⁹, Christian W Kohler¹⁸, Dirk Hasenclever¹⁹, Markus Kreuz¹⁹, Markus Loeffler¹⁹, Maciej Rosolowski¹⁹, Rainer Spang¹⁸. **Project coordination:** Benjamin Stürzenhofecker¹³, Lorenz Trümper¹³, Maren Wehner¹³. **Steering committee:** Markus Loeffler¹⁹, Reiner Siebert¹⁰, Harald Stein⁵, Lorenz Trümper¹³.

¹Institute of Pathology, University Hospital of Ulm, Germany, ²Institute of Pathology, University Hospital Schleswig-Holstein Campus Lübeck, Germany, ³Institute of Pathology, Kantonsspital St. Gallen, Switzerland, ⁴Institute of Pathology, University Hospital of Frankfurt, Germany, ⁵Institute of Pathology, Campus Benjamin Franklin, Charité–Universitäts-medizin Berlin, Germany, ⁶Institute of Hematopathology, University Hospital Schleswig-Holstein Campus Kiel/Christian-Albrechts University Kiel, Germany, ⁷Institute of Pathology, University of Würzburg, Germany, ⁸University Medical Center Hamburg-Eppendorf, Hamburg, Germany, ⁹Department of Hematology, Oncology and Tumor Immunology, University Medical Center Charité, Germany, ¹⁰Institute of Human Genetics, University Hospital Schleswig-Holstein Campus Kiel/Christian-Albrechts University Kiel, Germany, ¹¹Division of Pediatric Endocrinology and Diabetes, Department of Pediatrics, University Hospital Schleswig-Holstein Campus Kiel/Christian-Albrechts University Kiel, Germany, ¹²Institute for Cell Biology (Tumor Research), University of Duisburg-Essen, Germany, ¹³Department of Hematology and Oncology, Georg-August University of Göttingen, Germany, ¹⁴German Cancer Research Center (DKFZ), Heidelberg, Germany, ¹⁵Second Medical Department, University Hospital Schleswig-Holstein Campus Kiel/Christian-Albrechts University Kiel, Germany, ¹⁶Klinikum Esslingen, Esslingen, Germany, ¹⁷Department of Pediatrics I, Georg-August University of Göttingen, Germany, ¹⁸Institute of Functional Genomics, University of Regensburg, Germany, ¹⁹Institute for Medical Informatics, Statistics and Epidemiology, University of Leipzig, Germany ²⁰ Institute of Clinical Pathology, Robert-Bosch-Krankenhaus, Stuttgart, Germany.

II. Supplemental Material and Methods

Lymphoma samples

Lymphoma samples were derived from the Molecular Mechanisms in Malignant Lymphoma (MMML) cohort and a Polish cohort (Cytogenetic Laboratory The Maria Skłodowska-Curie Memorial Institute and Oncology Centre, Warsaw).^{1,2} Additional samples were collected from single diagnostic institutions. Molecular profiling of the cases included in the MMML cohort has been published recently.³

Cohort 1: Lymphomas called by both GEP classifiers (mBL and BL-PAP classifiers) Burkitt Lymphomas (n=59)

In order to identify *MYC*-negative lymphomas with a BL gene expression profiling (GEP), two independently developed gene expression classifiers, the molecular-BL (mBL) index³ and the BL-pathway activation pattern (BL-PAP classifier)⁴ were applied to a cohort of 753 previously characterized lymphomas from the Molecular Mechanisms in Malignant Lymphoma (MMML) Network. The two algorithms selected a total of 59 BL by GEP (Cohort 1). Two of these cases lacked a *MYC* translocation and were thus considered true *MYC*-negative BL.

Cohort 2: High-grade B-cell lymphomas and cell lines with features of BL, MYC negative (n=14)

Twelve *MYC*-negative lymphomas were included for cytogenetic and genetic analyses, five of which were previously reported.^{1,5,6} Of the total of 12 cases, eleven were included in the cohort 2 based on the diagnosis of BL/high-grade B-cell lymphoma and *MYC* break negativity and/or presence of 11q aberration. Cases 1-3 were collected from the Institute of Human Genetics, Kiel, cases 4-7 from the Polish study,^{1,2} and cases 8-9 and 11-12 from other institutions (National Institute of Health Bethesda, Institute Biology Grenoble, Institute of Pathology Tübingen). The diagnosis of BL was based on morphological criteria and the typical immunophenotype CD20+/CD10+/BCL2-/Ki67>90 (Table 1 and supplemental Table 2)(Klapper and Szczepanowski, unpublished).

The remaining case (case 10) was recruited from a recently published study on pediatric follicular lymphoma⁶ because of the prior knowledge of 11q-gain/loss pattern by CGH-array. This case simultaneously displayed follicular and diffuse growth pattern. Although its cytology

showed features of BL, it was classified as follicular lymphoma grade 3 (minor component) with simultaneous diffuse large B-cell lymphoma (major compartment) and it is because of this that was included in the previous series of pediatric lymphomas already published (supplemental Figure 1).

Finally HT and SU-DHL-5 cell lines (www.dsmz.de) were selected because they were negative for *BCL2* and *MYC* breaks and had cytogenetic evidences of the 11q-gain/loss pattern. Karpas-422 carrying also 11q-gain/loss pattern was excluded as a potential model because of the presence of t(14;18). Two additional cases from the Polish cohort that showed features resembling the other cases included in the present study (CD20+, CD10+, BCL6+, BCL2-, Ki67 100%) (cases 9 and 10 from Rymkiewicz et al.²) were initially included in the present but failed copy number (CN) analyses due to bad DNA quality and were therefore not further followed (data not shown). All biopsy specimens were evaluated by at least two hematopathologists (WK and IO, ESJ, PA or GR) according to the WHO classification⁷ (Table 1 and supplemental Table 2). Minimal regions of gain and loss in chromosome 11q were defined in this series (hg18).

Cohort 3: MMML cases with 11q gain/loss pattern determined by CGH-array (n=6)

A total of 514 MMML cases with available comparative genomic hybridization (CGH)-array data were screened for aberrations in the minimal regions previously described in the cohort 2. The region of gain was covered with 15 clones in the CGH-array whereas the region of loss had 8 clones. Those cases showing at least a partial gain and a partial loss within these regions were selected. The cases displaying non-mBL GEP were excluded. Excluding one relapse sample and one case of *IG/MYC*-positive mBL, *IGH/BCL2*-positive diffuse large B-cell lymphoma (DLBCL) and *BCL6* break-positive DLBCL, a total of six cases in which the 11q-gain/loss pattern could have been the initial event were selected. Gene expression, immunohistochemical and genetic features of these cases were compared with two different sets of reference samples. First set included all samples that exhibited mBL like GEP, *IG-MYC* positivity (n=46). The second set was comprised of DLBCL samples (n=198). All cases selected had not aberrations in the minimal 11q regions. Therefore, the probability of having one “true case” with the typical 11 pattern in the control cohort was very low.

Institutional Review Board approval

This study was performed as part of the MMML Network Project of the Deutsche Krebshilfe for which approval was obtained by the Institutional Review Board of the Medical Faculty Kiel under 403/05 as well as the study central. The protocols of the Berlin-Frankfurt-Münster (BFM) clinical trials have also been approved by central and local review boards.

FISH

The Digital image acquisition, processing, and evaluation were performed using ISIS digital image analysis system version 5.0 (Metasystems, Altlussheim, Germany). Methods on cases 4-7 have been previously published.¹

For FISH analyses, commercially available *MYC* BAP, *BCL6* BAP, *BCL2* BAP, *IGH* BAP, *MALT* BAP, *CCND1* BAP, *IGH/MYC/CEP8* and *IGH/CCND1* (all Abbott/Vysis, Downers Grove, IL) and the previously published probes *MYC* BAP 1,³ *MYC* BAP 2,³ FDX (+LSI ATM/CEP11)⁸ were used. In order to detect the deletion of chromosome 11q23~24 by FISH, a probe consisting of CEP11 (CEP11 [D11Z1, Spectrum aqua, Abbot, IL, USA]), RP11-453I14 containing the genes *PKN0X2* and *FEZ1* at 11q24.1 [Spectrum Orange] and RP11-349F17 containing the *NTM* gene at 11q25 [Spectrum Green]) was designed. FISH was observed according to standard procedures. The digital image acquisition, processing, and evaluation were performed using ISIS digital image analysis system version 5.0 (Metasystems, Altlussheim, Germany). FISH methods on samples 4-7 have been previously published.¹

DNA extraction

DNA extraction from the lymph node, paraffin material or cells in fixative was performed using standard protocols. DNA from SU-DHL-5 and HT cell lines (provided by DSMZ) was extracted from cultured cells.

Copy number analyses

GeneChip Mapping SNP 6.0 (Affymetrix, Santa Clara, CA) was used in cases 1-3 and 8 as previously described.⁹ Cases 4-7 and 9-12 were analyzed using the Agilent Human CGH Microarray platform (244K, only case 9 on 180K; Agilent Technologies, Santa Clara, CA) due to methodological requirements for formalin fixed paraffin embedded (FFPE) tissues. Genotyping Console (Affymetrix inc) was used to analyze copy number changes of SNP 6.0 array whereas Agilent arrays were analyzed using DNA Analytics (Agilent Technologies inc.) and/or Nexus CN 6.0 Discovery Edition (BioDiscovery, El Segundo, CA). Gains and losses on MPI samples (MMML Cohort) were analyzed as previously described.¹⁰ Additionally, the chromosome 11 was analyzed in all samples from the 'cohort 2' and 'cohort 3' (except MPI-315 and MPI-382) using Nexus 6.0 beta Discovery Edition (BioDiscovery, El Segundo, CA). Genetic complexity was defined as the number of CN aberrations per tumor sample.

Mutational analyses

PCR and direct sequencing of the PCR products were performed using the Big Dye Terminator v1.1 Cycle Sequencing Kit and the 3100-Avant Genetic Analyzer. Primers are summarized in supplemental Table 3. Polymorphic variants referenced in NCBI dbSNP Build 132 (<http://www.ncbi.nlm.nih.gov/projects/SNP/>) and 1000 genomes Project (<http://www.1000genomes.org/page.php>) were excluded. Non-synonymous mutations were tested for their functional consequences *in silico* by using different aminoacid substitution prediction algorithms, including SIFT (Sorting Intolerant From Tolerant) and PolyPhen-2 (Polymorphism Phenotyping).

Bisulfite pyrosequencing analyses

Methylation levels of hsa-mir-34b were studied in cases 1-7 from cohort 2 and SU-DHL-5 cell line, and in six *MYC*-positive BL and three *MYC*-positive BL cell lines (Ca-46, Daudi, Raji).

Bisulfite conversion and pyrosequencing was performed according to standard methods. The results were evaluated with the analysis software Pyro Q-CpG 1.0.9 (Biotage AB, Uppsala, Sweden), which was also used to quantify the percentage of methylated cytosines at the

analyzed CpG sites. All assays were optimized and validated using one complete methylated commercial available DNA (Millipore, Schwalbach, Germany) as positive control and an unmethylated pooled DNA isolated from 10 male and female controls as negative control. Primer sequences are shown in supplemental Table 3. Heterogeneous methylation patterns of hsa-mir-34b were found in the seven cases from the cohort 2 (Supplemental Figure 3). Cases 1, 3 and 7 displayed low levels of methylation (mean: 7, 7 and 3.5% respectively), whereas cases 2, 4, 5 and 6 showed higher levels of methylation (mean: 33, 36, 41 and 45%, respectively). The SU-DHL-5 cell line presented high levels of methylation (mean: 92%), similarly to the *IG-MYC*-positive BL cell lines (mean: 87%), and one primary case *IG-MYC*-positive BL (mean: 66%).

Exome sequencing data processing and Single Nucleotide Variant (SNV) and Small Indel Detection

For each sequencing lane, read pairs were mapped to the human reference genome (hg19, NCBI build 37.1, downloaded from the UCSC genome browser at <http://genome.ucsc.edu/>) using BWA version 0.5.9-r16 with default parameters and maximum insert size set to 1 kb. Samtools¹¹ was used to generate a chromosomal coordinate-sorted BAM file. PCR duplicates were removed using Picard tools (version picard-1.48, <http://picard.sourceforge.net>). Only uniquely aligned reads (minimum mapping quality of 1) overlapping on-target regions were considered for downstream analysis. Coverage calculations following duplicate removal considered all informative bases of the reference genome (excluding Ns). A mean Phred-scaled base quality of at least 25 across the length of the read was required. Detection of single nucleotide variants (SNVs) and small indels was done as described before.^{12,13} Filtered calls were functionally annotated using Annovar¹⁴ gene annotation and annotated for overlaps with dbSNP build 135 SNPs and variants from the 1000 Genomes project using BED Tools.¹⁵

Gene expression analyses

To evaluate the impact of 11q alterations in the GEP, differential gene expression analysis was performed using linear models for microarrays as implemented in the Bioconductor package

limma¹⁶ version 3.8.0. False discovery rates (FDR) were calculated according to Benjamini and Hochberg.¹⁷ Lists of differentially expressed genes were generated such that the FDR of the entire list is below .05.

To evaluate the direct impact of CN alterations, expression levels of genes within the minimal gained and lost region on chromosome 11 were compared between lymphomas with 11q gain/loss pattern and control groups.

The expression levels were compared by Student's t-test using R package multitest.¹⁸ A FDR cut-off of 0.1 was applied adjusting for the number of probesets within gain and loss region separately.

The differentially expressed genes between 11q-gain/loss and DLBCL or BL were investigated for significant over-representation by a hypergeometric test. Hereby, a list of differential genes is tested against a given set of genes contributing to particular Gene Ontology (GO) term which in turn is a subset of a GO category. A GO term is termed significant if the individual hypergeometric test results in a P-value below .05. Correction for multiple testing was performed by adjusting the P-values according to the procedure of Benjamini-Hochberg.¹⁷ The three GO categories - Molecular Function (MF), Biological Process (BP) and Cellular Component (CC) with their respective GO term - were tested separately.

MicroRNAs expression analysis

Test for overrepresentation of microRNA (miRNA) targets within a list of differentially expressed genes was performed in multiple hypergeometric tests as implemented in the HTSanalyzeR package (version 2.8.0).¹⁹ In this setting, the 'universe' is represented by the entire amount of probe sets on the hg133A chip (n=22283), whereas the number of differentially expressed genes constitute the 'observed hits'. We use the miRNA target sets within the gene set collection 'C3-motif gene sets' provided by the Broad Institute (<http://www.broadinstitute.org>), consisting of a total of 221 miRNA target gene sets. As a prerequisite, we require that each gene set contains at least 15 elements. Hence, a total of 213 gene sets remain for hypergeometric testing in this overrepresentation analysis. Each miRNA target set is tested for

enrichment in the list of differentially expressed genes. Statistical significance for overrepresentation of the individual miRNA target set ('expected hits') is assessed at the 0.05 level. Correction for multiple testing was performed by adjusting the *P*-values according to the procedure of Benjamini-Hochberg.¹⁷

Survival analysis

Survival curves were estimated by the Kaplan-Meier method. Survival differences were analyzed with the log-rank test. *P* values ≤ 0.05 were considered to indicate statistical significance.

Western Blot

Preparation of whole cell lysates from cell lines was done using RIPA buffer as described in the literature. Protein samples, suspended in water and 5x Lämmli buffer, were separated using Any kD Criterion TGX gels (Bio-Rad, München, Germany) and transferred to Immobilon-P Transfer Membrane (Millipore, Darmstadt, Germany). Membrane was blocked in 6% milk buffer-TBS-T for one hour at room temperature and afterwards incubated with the primary antibody PFAH1B2 mouse monoclonal antibody (M01A, clone 2FA-1C10, Abnova, Heidelberg, Germany). Lamin B1 (ab16048, Abcam, Cambridge, UK) and monoclonal anti- β -actin (Sigma-Aldrich, Steinheim, Germany) acted as reference genes. After washing, membranes were incubated for one hour at room temperature with HRP-conjugated donkey anti-rabbit IgG (DkxRb-003-DHRPX, ImmunoReagents Inc., Raleigh, USA) or donkey anti-mouse IgG (DkxMu-003-DHRPX, ImmunoReagents Inc.) and developed in Luminara Forte Western HRP Substrate (Millipore, Darmstadt, Germany). Signals were detected using Hyperfilm ECL (GE Healthcare, München, Germany).

Cell lines

Human BL cell lines BL-2, BL-41, BL-70, BLUE-1, Ca-46 and U-698-M, human DLBCL cell lines Karpas-422, SU-DHL-6 and SU-DHL-10 and cell lines with 11q-gain/loss pattern HT, SU-DHL-5

and MLMA (latter described by the Sanger Center) were obtained from the Leibniz Institute DSMZ-German Collection of Microorganisms and Cell Culture, except MLMA which was obtained from the Japanese Collection of Research Bioresources Cell Bank and cultivated according to the company's indications. Identity of cell lines was verified using Stem Elite ID (Promega, Mannheim, Germany).

III. Supplemental Results and Discussion

FISH validation

FISH analyses validated the array-based data and confirmed the presence of 11q gains and losses in the 'cohort 2' (Table 2). In contrast, the reported t(11;14) translocation in cases 6 and 7¹ was not confirmed by the use of a *CCND1* break apart probe. In case 3, the combination of R-banding and SNP-array data allowed the identification of the marker chromosome as a der(11)t(11;18)(q23;q21). The high frequency of 18q21-q22 breaks present in 4/12 cases is remarkable. A recent study has pointed *TCF4* gene, located in 18q21.2, as a candidate gene involved in an alternative mechanism to *ID3* mutations in the pathogenesis of BL.¹³ There was no evidence for involvement of the *MALT1* or *BCL2* oncogenes in the breakpoint region although two cases (1 and 3) presented gain of these genes.

hsa-mir-34b methylation levels

Recently, hsa-mir-34b was described to be down-regulated in BL cases that were negative for *MYC* translocation.²⁰ Remarkably, the hsa-mir-34b is located in 11q23.1 (chr11:110,888,873-110,888,956bp, hg18) and, thus, in the recurrently gained rather than the lost region. Thus, we analyzed the DNA-methylation of hsa-mir-34b. Heterogeneous methylation patterns of hsa-mir-34b were found in cases 1-7 from the cohort 2 (supplemental Figure 3). Additionally, we found no significant enrichment of hsa-mir-34b annotated target genes (Molecular Signatures Database, MSigDB) among the genes that were differentially expressed between cases with the 11q-gain/loss pattern and *Ig-MYC*-positive mBL, nor between these cases and DLBCL.

Supplemental discussion

Screening the Mitelman (<http://cgap.nci.nih.gov/Chromosomes/Mitelman>) and Progenetix database (www.Progenetix.org) (17th September 2012) for pediatric lymphomas, 10 out of 31 cases (32%) diagnosed as BL/Atypical without the t(8;14) translocation or variants presented alterations on chromosome 11

Specifically, two carried the duplication dup(11)(q13q23) and four presented additions at 11q23 or add(11)(q?).²¹⁻²⁴ On the other hand, *Pienkowska-Grela et al* reported an inversion of the gained region 11q13-q23 in four *MYC*-negative cases with typical BL morphology.¹ We also confirmed this in one additional case. Whether this cytogenetic change juxtaposes regulatory elements with a putative proto-oncogene is unknown. Breakpoints between the regions of gain and loss were not conserved in this series, but all of them were placed near the common fragile site FRA11G and the rare fragile site FRA11B, both located at 11q23.²⁵ However, there was no evidence that breakpoints were directly affecting these fragile sites (supplemental Figure 4B).

Remarkably, the *ATM* gene which is assumed to be a tumor suppressor gene²⁶ was located in the region of gain in 13/19 samples. With the exception of case 1 (that was known to have the AT syndrome), in which additionally to the gain a simultaneous mutation and CNN-LOH was detected, clinically no evidence of AT or immunodeficiency was reported in the remaining cases. Moreover, exome sequencing failed to identify *ATM* mutations in the cell lines investigated rendering a major role of *ATM* in the aberration unlikely.

Regarding the *ETS1* mutational analysis, case 5 (mutation G331G) and case 7 (mutation E22K) displayed a low fraction of the mutated allele. Surprisingly, both cases also showed mutations in other exons in which the mutated allele was the predominant. These results together with the fact that these cases showed a deletion in 11q including the *ETS1* gene, lead us to speculate about the possible presence of subclones. Moreover, our attempts to model the effect of the mutations yielded no striking results due to the low number of mutations found in our series, and the fact that none of the point mutations were within resolved three-dimensional structures. However, both P→A (case 5) and E→K (case 7) lie at the N-terminus of the protein, and are close (in two of three isoforms of *ETS1*) to the Pnt domain which could influence the interaction with other proteins.²⁷ In contrast, the Y→X/del (case 8) which removes the DNA binding domain, and the S→F mutation, which lays 10 residues N-terminal to this domain, are more likely to influence the DNA binding.

Concerning the genes involved in the frequent co-deletions of 6q observed in this series, the *EPHA7* gene (6q16) has been recently described as a tumor suppressor in follicular lymphoma with interesting therapeutical involvements.²⁸ Moreover, inactivating mutations in *PRDM1* (6q21) that result in the generation of a severely truncated non functional protein, are found in about 20% of the DLBCLs.²⁹

IV. Supplemental Tables

Supplemental Table 1. Case selection of Cohort 2.

Case	Morphologic features	IHC features	MYC-negativity	11q alteration by cytogenetics	11q-gain/loss pattern by arrays	Reference paper
Case 1	x	x	x			
Case 2	x	x	x			
Case 3	x	x	x			
Case 4	x	x	x	x		Pienkowska-Grela et al ¹
Case 5	x	x	x	x		Pienkowska-Grela et al ¹
Case 6	x	x	x	x		Pienkowska-Grela et al ¹
Case 7	x	x	x	x		Pienkowska-Grela et al ¹
Case 8			x	x		
Case 9	x	x	x			
Case 10			x		x	Oschlies et al/ Martin-Guerrero et al ^{5,6}
Case 11	x	x	x			
Case 12	x	x	x			
HT			x	x		
SU-DHL-5			x	x		

*Case 10 displayed simultaneously a follicular and diffuse growth pattern. Although its cytology showed features of BL, it was classified as follicular lymphoma grade 3 (minor component) with simultaneous diffuse large B-cell lymphoma (major compartment).^{5,6}

BL: Burkitt Lymphoma; IHC: immunohistochemical.

Supplemental Table 2. Morphological characteristics of the samples included in the study (cohort 2 and cohort 3)

Case	Quality	Growth pattern	Cytology					Bystander
	morphologic quality	starry sky	cell size	cell polymorphism	cytoplasm	nuclear shape	Burkitt like-chromatin/nucleoli	bystander cells
Case 1/MPI-626	poor	na	na	Na	na	na	na	na
Case 2	good	1	1	1	1	1	2	1
Case 3	good	1	1	2	1	1	1	1
Case 4	good	1	1	1	1	1	1	1
Case 5	reduced	1	1	1	1	1	1	1
Case 6	poor	1	1	2	1	1	2	na
Case 7	good	1	1	1	1	1	1	1
Case 8	poor	2	1	1	na	1	1	1
Case 9	good	1	1	2	na	1	1	na
Case 10	good	1	1	1	1	1	1	1
Case 11	good	1	1	1	1	2	1	1
Case 12	good	1	1	1	1	1	1	1
MPI-078	good	1	1	1	1	2	2	1
MPI-086	poor	na	na	Na	na	na	na	na
MPI-148	reduced	1	1	1	1	1	2	1
MPI-315	reduced	2	2	1	1	1	2	1
MPI-382	good	1	1	1	1	2	1	1

Morphological scoring criteria: in bold=pro-Burkitt/ italics=against Burkitt

growth pattern

starry sky

1= yes (cohesive growth, tingible body macrophages) , 2= no

cytology

cell size

1= medium (nuclei similar or smaller than those of histiocytes), 2= large (nuclei larger than those of histiocytes)

cell polymorphism

1= no, 2=yes

cytoplasm

1= narrow, 2= abundant

nuclear shape

1= round, 2= irregular

Burkitt-like

chromatin/nucleoli

1= yes (moderately dense chromatin, inconspicuous nucleoli) , 2= no (Similar to other lymphomas Centroblastic-like, Immunoblastic-like, Lymphoblastic-like)

bystander

bystander cells

1= scattered, 2= moderate (clusters >10 cells), 3= abundant (outweighing lymphoma cells)

na: not available

Supplemental Table 3. Primer information for mutational and methylation analysis

Exon	Sequence (5'-3')	PCR product length (bp)
FLI1_exon1_F	TGTAACCGGGTCAATGTGTG	176
FLI1_exon1_R	GAGAGAGGCCACGTCTTCC	
FLI1_exon2_F	TGAAGAGTGACACTGGGCTTT	298
FLI1_exon2_R	TTTGTGCCTTCCCCCAAT	
FLI1_exon3_F	GCCTCTGGGCTTTGTCTCTT	206
FLI1_exon3_R	GCAGCCTGGTTCTCGAATTA	
FLI1_exon4_F	TGCTAACAACGTCTTCTCCTCT	250
FLI1_exon4_R	GGTACTTGGGCGGCACTTAC	
FLI1_exon5_F	TCCCTCCTCATGTCATCTCC	235
FLI1_exon5_R	CAAGCTGGTTTTCTGCAACA	
FLI1_exon6_F	GAAGCAGGCGATGCTAATGT	176
FLI1_exon6_R	CCTGTTCTCCAATCCTGTCC	
FLI1_exon7_F	TGCATTTCTTTCCCTCTTGC	136
FLI1_exon7_R	TCAACAACGTGCAGGAAGC	
FLI1_exon8_F	GGTTTTCTTATGGTTGGTACGG	220
FLI1_exon8_R	CCCCTCAGGTGTCTGGACT	
FLI1_exon9a_F	TCTCTGGGCTGAGGTGTTCT	214
FLI1_exon9a_R	ATTCATGTTGGGCTTGCTTT	
FLI1_exon9b_F	AAAGCAAGCCCAACATGAAT	264
FLI1_exon9b_R	AGGAAGTGACAGGCATGGAG	
FLI1_exon9c_F	CTCCATGCCTGTCACTTCT	212
FLI1_exon9c_R	TGTTGAGTCCAAAGCATCCA	
ETS1_2_F	AAGGTTTCGTGTCTTCCTTGTG	273
ETS1_2_R	AGTTCAGGTTCCCTGGCTTCTC	
ETS1_3_F	AAACAAGAGTTGGCTCTGTTCTG	365
ETS1_3_R	GAAAGAATGCAGCCCTCATC	
ETS1_4_F	AAGAAAGTCGATTTCCCC	308
ETS1_4_R	CTCCTGAAGAAATGCACCG	
ETS1_5_F	GCCTTCTTACAGCCCATTTG	275
ETS1_5_R	CAGGTGAGAAAATGTGTCTTCC	
ETS1_6_F	GTGTCCTCTCTGAGGCTTGG	353
ETS1_6_R	CCCACCATTGGGTGAGC	
ETS1_7_F	CCAAGATCCTTTTAGGCCAAG	232
ETS1_7_R	GAAGGAGCCTGAGATTCACTG	
ETS1_8_F	GCTTGTCCCACATCATAGGG	476
ETS1_8_R	AGATGGGAAGGCTGAACTG	
ETS1_9_F	AATCTGTCCTCCATAAGAGGG	419
ETS1_9_R	CCTCCAGGACCCACC	
ETS1_10_F	TGGGGATTAGCTGCGTAGAG	276
ETS1_10_R	CTGGAACACGTCATTCAGGC	
ETS1_11_F	TGGGTATAGCATAGGCATAGAAAC	375
ETS1_11_R	TTCAGAGTCCAACCAACACG	
hsa-mir-34b_PS-FP	GTGTTTTGTTTTGATGGTAGTGGAGTTAGTGATTGTAATT	185
hsa-mir-34b_PS-RP	Biotin-CCAACCATAATAAAACCTCCCCCATAAAAATAAAATC	
hsa-mir-34b_PS-seq	ATAATTAGTTAATGATATTGTTTAT	

F: forward; R: reverse; bp: base pairs

Supplemental Table 4. Global table of copy number alterations (cohort 2 + cohort 3)

Case No.	Alteration	Start*	Stop*	Size (Mb)
COHORT 2				
Case 1				
	ampl 1q21.2-q21.2	148685774	148941059	0.26
	gain 2q21.3-q22.1	136125291	137663460	1.54
	gain 3q27.3-q28	189042530	191120493	2.08
	gain 3q29	195204051	199293383	4.09
	loss 4q21.21-q22.1	81489318	93269598	11.78
	gain 4q23-q24	102280753	104354915	2.07
	loss 6q13-q22.2	74993911	118220610	43.23
	gain 7p21.3	11240265	11413684	0.17
	gain 7q34-qter	140514593	158812469	18.30
	gain 8q23.1-q24.22	109813698	134442702	24.63
	gain 11q12.1-q23.3	59689284	119681559	59.99
	loss 11q23.3-qter	119707054	134452384	14.74
	ampl 12q12-q13.12	42863301	47443460	4.58
	gain 13q22.3-q33.2	76775526	104991992	28.22
	loss 13q33.2-qter	104993812	114125098	9.13
	loss 14q32.33	105149735	105346366	0.20
	gain 14q32.33	105613310	106247258	0.63
	gain 18q12.1	28544883	28653780	0.11
	gain 18q12.3-q22.1	39073072	60244448	21.17
	ampl 18q21.1-q22.1	45653539	60244448	14.59
	loss 18q22.1-qter	60252055	76116029	15.86
Case 2				
	gain 1p34.3	35106424	35228372	0.12
	gain 1p14	70156025	70275477	0.12
	loss 2q32.1	188942379	189076699	0.13
	gain 3q21.3	131213377	131327230	0.11
	gain 3q25.32	159758744	159865413	0.11
	gain 3q27.1	184795403	184968811	0.17
	gain 3q29	199232833	199380402	0.15
	gain 7p21.3	11040165	11203172	0.16
	gain 7p15.2	27081809	27213804	0.13
	gain 7p12.3	47931639	48054390	0.12
	gain 7q22.1	98389903	98512841	0.12
	gain 8q24.3	141603380	141717824	0.11
	gain 8q24.3	145924264	146099639	0.18
	gain 10p15.3	62797	903825	0.84
	loss 10q23.2-q23.32	89293858	94120662	4.83
	gain 11q12.1-q23.3	57719840	119962965	62.24

	ampl 11q23.3	115475451	119962965	4.49
	loss 11q23.3-qter	119973847	134452384	14.48
	gain 12q24.33	131911167	132064588	0.15
	gain 13q31.3	90765745	91159861	0.39
	gain 14q32.33	105190672	105391419	0.20
	loss 14q32.33	105601397	105867261	0.27
	gain 14q32.33	106255229	106356482	0.10
	gain 15q15.2	41054903	41376506	0.32
	gain 18q21.2	49304445	51292535	1.99
Case 3				
	gain 1q32.1	201704327	202879427	1.18
	gain 3pter-q13.11	237715	105278073	105.04
	ampl 3q12.1-q13.11	99899652	105278073	5.38
	loss 3q13.11-q22.1	105545355	135653661	30.11
	gain 3q22.1-qter	135661150	199380402	63.72
	loss 6q14.3-q24.2	86506785	145521066	59.01
	gain 7p22.2	2375274	2757211	0.38
	loss 8q12.3-q13.2	63919515	69504641	5.59
	gain 10q24.32-q26.3	103736630	135356682	31.62
	loss 11p11.2	44661682	47027619	2.37
	loss 11q23.3-qter	120136046	134452384	14.31
	gain 14q32.33	105196431	106147535	0.95
	loss 15q15.3-q21.1	42638536	42851097	0.21
	gain 18q21.1-q23	43506879	76021279	32.51
	gain 22q12.2	29401354	30291713	0.89
	loss Xp22.33-qter	297864	153177486	152.88
Case 4				
	gain 11q13.1-q23.3	65143127	119833054	54.69
	loss 11q23.3-qter	119874121	134452384	14.58
Case 5				
	gain 7q34-qter	137991760	158811327	20.82
	gain 11q13.4-q24.1	72339170	123014463	50.67
	loss 11q24.1-qter	123021426	134445937	11.42
	gain 12 whole chromosome			
	loss 13q14.3-qter	52139320	114123908	61.98
	loss 17q24.3	65705035	66940878	1.24
Case 6				
	gain 11q13.1-q23.3	64641564	119519782	54.88
	ampl 11q23.3	115922770	119519782	3.60
	loss 11q23.3-qter	119538171	134452384	14.91
	gain 19pter-p13.2	231880	7573593	7.34
Case 7				

	gain 11q13.1-q24.1	63779666	121499506	57.72
	loss 11q24.1-qter	121516192	134452384	12.94
	gain 12 whole chromosome			
Case 8				
	gain 7q31.1-qter	113416517	1588214241	45.40
	loss 9q21.11-q31.1	70196160	103751610	33.56
	gain 11q12.1-q24.2	58680791	126956874	68.28
	loss 11q24.2-qter	126977015	135006516	8.03
	gain 12pter-p12.2	1	20891006	20.84
	loss 12p12.2-p12.1	20891875	21307564	0.41
	gain 12p12.1-qter	21445461	132289534	110.84
Case 9				
	loss 2q14.3-q31.1	127122505	170503003	43.38
	gain 11q13.1-q23.3	66885327	120439037	53.37
	ampl 11q14.3-q23.3	92942578	120439037	27.50
	loss 11q23.3-qter	120445525	134452384	14.01
	homoz loss 11q24.2-q24.3	127322011	128846569	1.52
Case 10				
	gain 10	0	135374737	135.37
	gain 11q12.1-q23.3	58553066	118931293	60.38
	ampl 11q23.3	117107361	118883140	1.78
	loss 11q23.3-qter	118941150	134452384	15.51
Case 11				
	loss 7p22.2-p22.1	4415401	6829674	2.41
	loss 7q11.21-q11.22	61469275	68687083	7.22
	loss 7q11.22 - q11.23	70246922	75936506	5.69
	loss 7q21.3 - q22.3	94515368	105073913	10.56
	gain 8q24.13 - q24.23	125040422	138214195	13.17
	gain 11q13.1-q23.3	66430840	117939359	51.51
	loss 11q23.3-qter	117999595	134452384	16.45
	loss 19 whole chromosome			
Case 12				
	gain 11q12.1-q23.3	58608311	118452523	59.84
	loss 11q23.3-q25	118452523	134452384	16.00
SU-DHL-5				
	loss 1p36.32-p36.31	4371886	6440078	2.07
	loss 3q13.31	117721944	118017064	0.30
	loss 6pter-p22.1	94649	27222031	27.13
	loss 6q13-qter	74812911	170824447	96.01
	loss 11q23.2	114373214	114527878	0.15
	gain 11q23.2-q23.3	114530818	117966632	3.44
	loss 11q23.3-qter	117980123	134452384	16.47

	gain 12pter-q13.11	20691	46498049	46.48
	gain 13q31.3	90128337	91984789	1.86
	loss 16p13.3	3567612	4346884	0.78
	gain 19pter-p13.2	41898	6181751	6.14
HT				
	loss 2p25.3-p24.1	0	22609737	22.6
	loss 2p23.3	25767848	27139364	1.37
	ampl 2p23.1	30621717	30833375	0.21
	loss 2p23.1-p22.3	30836938	32537678	1.70
	ampl 2p22.3	32541543	33682722	1.14
	loss 2p22.3-p16.2	33687378	53916677	20.23
	gain 2p16.2-16.1	53924856	55183842	1.26
	loss 2p16.1-p15	55194316	61240592	6.04
	ampl 2p15	61244295	61662952	0.42
	loss 2p15-p12	62359975	83064902	20.70
	loss 2q13-q24.1	111902315	155664643	43.76
	loss 4pter-p12	0	48664347	48.66
	gain 10q21.1-q22.2	55364108	75247849	19.88
	ampl 11q14.3	88144006	89725365	1.58
	ampl 11q21	93876132	95108752	1.23
	ampl 11q22.1-q22.3	99835629	103320029	3.48
	ampl 11q23.2	106152997	113742929	7.59
	loss 11q23.2	113768098	114062057	0.29
	ampl 11q23.2-q23.3	114068752	118677633	4.61
	loss 11q23.3-qter	118679677	134452384	15.77
COHORT 3				
MPI-078				
	loss 6q14.1-q21	80482703	110738634	30.26
	loss 9p22.3-p22.1	16388202	18522051	2.13
	gain 11q22.1-q23.3	88473456	118296472	29.82
	ampl11q23.3	117017708	118296472	1.28
	loss 11q23.3-qter	118322247	134452384	16.13
	gain 12pter-q13.11	152505	46627459	46.47
	loss 13q31.3-qter	92499761	113932806	21.43
	gain 14q11.2-q31.3	19570792	88183880	68.61
	loss 14q32.12-qter	91389759	105139439	13.75
	loss 15q11.2	18959894	20286790	1.33
	gain 16p12.3-p11.2	18586418	30940331	12.35
	loss Yp11.31-q11.23	2845473	26798441	23.95
MPI-086				
	loss 1p31.1	78953798	83496487	4.54

	gain 8 whole chromosome			
	loss 9p22.2-p22.1	16995146	18522051	1.53
	loss 9p21.3-p21.2	21899259	25853240	3.95
	gain 11q22.1-q24.1	86049526	115060942	29.01
	loss 11q23-q23.3	115205059	115933496	0.73
	gain 11q23.3-q24.1	115933496	122263962	6.33
	loss 11q24.1-qter	122263962	134452384	12.19
	gain 12q13.11-q14.1	46569188	56455000	9.89
	gain 12q23.2-q24.32	101524012	124849229	23.33
	gain 19 whole chromosome			
	loss 20q13.2-q13.31	51561511	54897122	3.34
MPI-148				
	gain 11q12.2-q24.1	60068023	122862967	62.79
	loss 11q24.1-qter	122867926	134452384	11.58
MPI-315				
	gain 1q21.1-q21.3	143613589	153292828	9.68
	loss 1q32.1-qter	202748873	245280397	42.53
	loss 2pter-p16.1	2250133	60403212	58.15
	gain 2p16.1-p15	60403013	61380667	0.98
	loss 3q13.31-q21.2	117048246	127483269	10.44
	loss 4q12-q12	54654383	54825096	0.17
	loss 4q13.3-q33	74788409	172115114	97.33
	loss 5p15.32-p13.2	5500091	35078858	29.58
	gain 6pter-p25.2	352879	3427043	3.07
	loss 6p25.1-p22.3	5800622	20018591	14.22
	gain 6p22.3-p21.1	20523579	45164736	24.64
	loss 6p12.3-qter	46918395	170799954	123.88
	gain 7 whole chromosome			
	loss 8p23.3-p11.21	20005607	42333716	22.33
	loss 9p24.1-p13.2	8398602	36897415	28.50
	gain 11q23.2-q23.3	115397542	118898368	3.50
	loss 11q23.3-qter	118950353	133706190	14.76
	gain 12q13.3-q13.3	50803968	52714396	1.91
	gain 12q22-q22	92645921	93711389	1.07
	loss 12q22-q24.1	94176856	113932806	19.76
	loss 15q11.2-qter	18959894	100036184	81.08
	loss 16pter-pter	266994	4851459	4.58
	loss 17pter-p11.2	343377	19021902	18.68
	loss 17q22-qter	52616469	78374826	25.76
	loss 18pter-p11.22	168384	9587352	9.42
	loss 22q11.21-qter	20261797	48869117	28.61
	gain Xq22.1-qter	98412392	154482340	56.07

MPI-382	gain Yp11.31-q11.23	2845473	26798441	23.95
	gain 1q21.1-qter	143613589	245280397	101.67
	loss 6q14.1-qter	80482703	170799900	90.32
	gain 11q22.3-q24.2	104674037	125152144	20.48
	loss 11q24.2-qter	126924590	133706190	6.78
	gain 13q14.3-qter	50328519	113932806	63.60
	loss 17pter-p11.2	343377	2023038	1.68
	loss 18pter-p11.22	168384	10203413	10.04
	loss 20q13.3-q13.2	48590356	49575686	0.99
	gain Xp11.4-p11.1	41107931	57113775	16.01
MPI-626[†]	gain 2q33.1-33.1	200593235	201799587	1.21
	loss 6q14.1-q22.2	80482703	118016198	37.53
	gain 7q34-q35	140911726	143375452	2.46
	gain 7q35-qter	146949516	157754947	10.81
	gain 11q12.2-q14.1	59931009	78206821	18.28
	gain 11q23.2-q23.3	114823728	119763552	4.94
	loss 11q23.3-qter	119773351	133706190	13.93
	gain 12q13.11-13.11	44606441	47291634	2.69
	loss 13q33.3-qter	106527417	113932806	7.41
	gain 18q12.3-q22.1	41216561	60139386	18.92
	loss 18q22.1-qter	60417711	74870960	14.45

*Annotation hg18/NCBI 36.1; [†]Case MPI-626 corresponds to case 1 from cohort 2.

Supplemental Table 5. Regions of gain/amplification and loss in chromosome 11q and minimal region according to hg18/NCBI 36.1 (cohort 2 and cohort 3)

Analyzed using DNA Analytics/Genotyping Console/Nexus				Analyzed using Nexus			
Case	Alteration	Start	End	Case	Alteration	Start	End
1	gain 11q12.2-q23.3	59744929	119703938	1	gain 11q12.1-q23.3	59689284	119681559
2	gain 11q12.1-q23.3	57743468	119935705	2	gain 11q12.1-q23.3	57719840	119962965
2	ampl 11q23.3	115501782	119935705	2	ampl 11q23.3	115475451	119962965
4	gain 11q13.4-q23.3	72233510	118474726	4	gain 11q13.1-q23.3	65143127	119833054
5	gain 11q13.4-q24.1	72472183	122987191	5	gain 11q13.4-q24.1	72339170	123014463
6	gain 11q13.1-q23.3	64320482	119515306	6	gain 11q13.1-q23.3	64641564	119519782
6	ampl 11q23.3	115930770	119515306	6	ampl 11q23.3	115922770	119519782
7	gain 11q13.3-q24.1	70490787	121042870	7	gain 11q13.1-q24.1	63779666	121499506
8	gain 11q12.1-q24.2	58437367	126462084	8	gain 11q12.1-q24.2	58680791	126956874
9	gain 11q13.1-q23.3	66841504	120212444	9	gain 11q13.1-q23.3	66885327	120439037
9	ampl 11q14.3-q23.3	89390459	120212444	9	ampl 11q21-q23.3	92942578	120439037
10	gain 11q12.1-q23.3	58686057	118931293	10	gain 11q12.1-q23.3	58553066	118883140
10	ampl 11q23.3	117207811	118931293	10	ampl 11q23.3	117107361	118883140
11	gain 11q13.1-q23.3	66537264	117930644	11	gain 11q13.1-q23.3	66375228	117939359
12	gain 11q12.1-q23	58608311	118452523	12	gain 11q12.1-q23	58608311	118452523
SU-DHL-5	gain 11q23.2-q23.3	114528073	117977645	SU-DHL-5	gain 11q23.2-q23.3	114530818	117966632
HT	ampl 11q14.3	88135598	89721310	HT	ampl 11q14.3	88144006	89725365
HT	gain 11q21	93878519	95107104	HT	ampl 11q21	93876132	95108752
HT	ampl 11q22.1-q22.3	99775174	103373313	HT	ampl 11q22.1-q22.3	99835629	103320029
HT	gain 11q22.3-q23.2	106159402	113765153	HT	ampl 11q23.2	106152997	113742929
HT	ampl 11q22.3-q23.2	107292911	113765153				
HT	ampl 11q23.2-q23.3	114062136	118676746	HT	ampl 11q23.2-q23.3	114068752	118677633
MPI-078	gain 11q22.1-q23.3	100393958	118220300	MPI-078	gain 11q14.3-q23.3	88473456	118296472
				MPI-078	ampl 11q23.3	117017708	118296472
MPI-086	gain 11q22.1-q24.1	100393958	122299458	MPI-086	gain 11q14.2-q23.2	86049526	115060942
				MPI-086	gain 11q23.3-q24.1	115933496	122263962
MPI-148	gain 11q12.2-q14.1	61393968	78206821	MPI-148	gain 11q12.2-q24.1	60068023	122862967
MPI-148	gain 11q23.3-q24.1	116204676	122299458				
MPI-315	gain 11q23.2-q23.3	115397542	118898368	MPI-315	not analyzed by Nexus		
MPI-382	gain 11q22.3-q24.2	104674037	125152144	MPI-382	not analyzed by Nexus		
MPI-626	gain 11q12.2-q14.1	59931009	78206821	MPI-626	not analyzed by Nexus		
MPI-626	gain 11q23.2-q23.3	114823728	119763552				
Minimal region of gain/amplification				Minimal regions of gain/amplification			
		Start	End			Start	End
MR gain		114528073	117930644	MR gain		114530818	117939359
MR ampl		117207811	117930644	MR ampl		117107361	117939359

Case	Alteration	Start	End	Case	Alteration	Start	End
1	loss 11q23.3-qter	119710170	134449982	1	loss 11q23.3-qter	119707054	134452384
2	loss 11q23.3-qter	119940234	134324199	2	loss 11q23.3-qter	119973847	134452384
3	loss 11q23.3-qter	120642730	134335292	3	loss 11q23.3-qter	120136046	134452384
4	loss 11q23.3-qter	119882984	134432465	4	loss 11q23.3-qter	119874121	134452384
5	loss 11q24.1-qter	122999748	134432465	5	loss 11q24.1-qter	123021426	134445937
6	loss 11q23.3-qter	119524200	134432465	6	loss 11q23.3-qter	119538171	134452384
7	loss 11q24.1-qter	121083826	134432324	7	loss 11q24.1-qter	121516192	134452384
8	loss 11q24.2-qter	126482225	134451988	8	loss 11q24.2-qter	126977015	135006516
9	loss 11q23.3-qter	120445552	134451988	9	loss 11q23.3-qter	120445525	134452384
9	homoz loss 11q24.2-q24.3	127322011	128846569	9	homoz loss 11q24.2-q24.3	127322011	128846569
10	loss 11q23.3-qter	118936999	134431956	10	loss 11q23.3-qter	118941150	134452384
11	loss 11q23.3-qter	117956255	134451988	11	loss 11q23.3-qter	117999595	134452384
12	loss 11q23.3-qter	118452523	134451988	12	loss 11q23.3-qter	118452523	134452384
SU-DHL-5	loss 11q23.3	114376008	114527684	SU-DHL-5	loss 11q23.2	114373214	114527878
SU-DHL-5	loss 11q23.3-qter	117982577	134449982	SU-DHL-5	loss 11q23.3-qter	117980123	134452384
HT	loss 11q23.2	113771043	114061954	HT	loss 11q23.2	113768098	114062057
HT	loss 11q23.3-qter	118681608	134449982	HT	loss 11q23.3-qter	118679677	134452384
MPI-078	loss 11q23.3-qter	118258492	133706190	MPI-078	loss 11q23.3-qter	118322247	134452384
MPI-086	loss 11q24.1-qter	123265158	133706190	MPI-086	loss 11q23.2-q23.3	115205059	115933496
MPI-148	loss 11q24.1-qter	123265158	133706190	MPI-086	loss 11q24.1-qter	122263962	134452384
MPI-315	loss 11q23.3-qter	118950353	133706190	MPI-148	loss 11q24.1-qter	122867926	134452384
MPI-382	loss 11q24.2-qter	126924590	133706190	MPI-315	not analyzed by nexus		
MPI-626	loss 11q23.3-qter	119773351	133706190	MPI-382	not analyzed by nexus		
MPI-626	loss 11q23.3-qter	119773351	133706190	MPI-626	not analyzed by nexus		
Minimal region of loss				Minimal region of loss			
		Start	End			Start	End
MR loss		126482225	134324199	MR loss		126977015	134445937
MR homoz loss		127322011	128846569	MR homoz loss		127322011	128846569

ampl: amplification; homoz loss: homozygous loss; MR: minimal region. Bold positions delineate minimal regions of gain and loss.

Supplemental Table 6. Comparison of immunohistochemical and genetic features between cases with 11q gain-loss pattern (cohort 3) (n=6) and *IG-MYC* mBL (n=46) and DLBCL (n=198). 11q samples and DLBCL controls were compared by Fishers exact test.

	<i>IG-MYC</i> positive mBL n=46	11q <i>MYC</i> -negative n=6	DLBCL n=198	<i>P</i> -value (11q vs DLBCL)
Gender	n (%)			
Female	11(24%)	1(17%)	89(45%)	
Male	35(76%)	5(83%)	108(55%)	
CD20				
Neg	0	1(17%)	11(6%)	
Pos	46(100%)	5(83%)	186(94%)	
CD10				
Neg	1(2%)	1(17%)	133(69%)	
Pos	43(98%)	5(83%)	59(31%)	<i>P</i> =.014
CD5				
Neg	41(93%)	5(100%)	158(86%)	
Pos	3(7%)	0(0%)	25(14%)	
BCL2				
Neg	37(86%)	4(80%)	33(17%)	<i>P</i> =.005
Pos	6(14%)	1(20%)	157(83%)	
BCL2INT				
0	34(81%)	4(80%)	20(11%)	<i>P</i> <.001
1	6(14%)	1(20%)	65(35%)	
2	1(2%)	0(0%)	71(38%)	
3	1(2%)	0(0%)	30(16%)	
BCL6				
Neg	2(5%)	0(0%)	39(21%)	
Pos	41(95%)	6(100%)	147(79%)	
MUM1				
Neg	23(56%)	3(60%)	53(28%)	
Pos	18(44%)	2(40%)	133(72%)	
HLADR				
Neg	10(24%)	2(40%)	30(17%)	
Pos	31(66%)	3(60%)	151(76%)	
KI67				
Low (<90)	3(7%)	1(17%)	145(76%)	
High (>90)	42(93%)	5(83%)	47(24%)	<i>P</i> =.005
MYC status				
<i>IG-MYC</i>	46(100%)	0(0%)	6(3%)	
Neg	0(0%)	6(100%)	179(90%)	
non- <i>IG-MYC</i>			13(7%)	
t(14;18)				
Neg	45(98%)	6(100%)	175(88%)	
Pos	1(2%)	0(0%)	23(12%)	
BCL6 break				
Neg	45(98%)	6(100%)	151(78%)	
Pos	0(0%)	0(0%)	43(22%)	
MALT1 break				
Neg	45(100%)	5(100%)	188(99%)	
Pos			1(1%)	
IGH break				

Neg	2(4%)	4(67%)	117(62%)	
Pos	44(96%)	2(33%)	73(38%)	
GEP				
GCB/ABC				
ABC	0(0%)	0(0%)	61(31%)	
GCB	41(89%)	6(100%)	88(44%)	<i>P</i> =.04
unclassified	5(11%)	0(0%)	49(25%)	
Molecular diagnosis				
intermediate	0(0%)	3(50%)	29(15%)	
mBL	46(100%)	3(50%)	0(0%)	<i>P</i> <.001
non-mBL	0(0%)	0(0%)	169(85%)	
COMAP				
BL-PAP	46(100%)	3(50%)	0(0%)	<i>P</i> <.001
mind-L	0(0%)	2(33%)	43(22%)	
PAP-1	0(0%)	1(17%)	84(42%)	
PAP-2	0(0%)	0(0%)	23(12%)	
PAP-3	0(0%)	0(0%)	26(13%)	
PAP-4	0(0%)	0(0%)	22(11%)	

The scoring for BCL2 intensity (int) is as follows: 1=weaker than T-cells, 2=equal than T-cells, 3= stronger than T-cells.

Supplemental Table 7. Differentially expressed genes between cases with 11q-gain/loss pattern (cohort 3) (n=6) and *IG-MYC* mBL (n=46)

Differentially expressed genes in the 11q minimal region of gain between cases with 11q-gain/loss pattern and <i>IG-MYC</i> BL						
affy_hg_u133a	symbol	description	logFC	adj.P.Val	gene expression status	Chr Band
204912_at	<i>IL10RA</i>	interleukin 10 receptor, alpha	1,678075	5,51E-09	upReg_in_11q	11q23
200054_at	<i>ZNF259</i>	zinc finger protein 259	0,527004	6,01E-06	upReg_in_11q	11q23.3
210160_at	<i>PAFAH1B2</i>	platelet-activating factor acetylhydrolase 1b, catalytic subunit 2 (30kDa)	0,356262	3,77E-05	upReg_in_11q	11q23
204251_s_at	<i>CEP164</i>	centrosomal protein 164kDa	0,307823	0,005803	upReg_in_11q	11q23.3
56256_at	<i>SIDT2</i>	SID1 transmembrane family, member 2	0,507588	0,034517	upReg_in_11q	11q23.3
218765_at	<i>SIDT2</i>	SID1 transmembrane family, member 2	0,285941	0,040985	upReg_in_11q	11q23.3
Differentially expressed genes in the 11q minimal region of loss between cases with 11q-gain/loss pattern and <i>IG-MYC</i> BL						
affy_hg_u133a	symbol	description	logFC	adj.P.Val	gene expression status	Chr Band
204236_at	<i>FLI1</i>	Friend leukemia virus integration 1	-0,94562	1,12E-05	downReg_in_11q	11q24.3
208703_s_at	<i>APLP2</i>	amyloid beta (A4) precursor-like protein 2	-0,99233	8,07E-05	downReg_in_11q	11q24
208248_x_at	<i>APLP2</i>	amyloid beta (A4) precursor-like protein 2	-0,85109	9,35E-05	downReg_in_11q	11q24
208704_x_at	<i>APLP2</i>	amyloid beta (A4) precursor-like protein 2	-0,80842	9,35E-05	downReg_in_11q	11q24
218491_s_at	<i>THYN1</i>	thymocyte nuclear protein 1	-0,62595	0,000474	downReg_in_11q	11q25
221669_s_at	<i>ACAD8</i>	acyl-CoA dehydrogenase family, member 8	-0,49925	0,001474	downReg_in_11q	11q25
212789_at	<i>NCAPD3</i>	non-SMC condensin II complex, subunit D3	-0,51814	0,001519	downReg_in_11q	11q25
213028_at	<i>NFRKB</i>	nuclear factor related to kappaB binding protein	-0,24125	0,001533	downReg_in_11q	11q25
210786_s_at	<i>FLI1</i>	Friend leukemia virus integration 1	-0,77575	0,002557	downReg_in_11q	11q24.3
202359_s_at	<i>SNX19</i>	sorting nexin 19	-0,27369	0,006075	downReg_in_11q	11q25
216905_s_at	<i>ST14</i>	suppression of tumorigenicity 14 (colon carcinoma)	-0,66041	0,006449	downReg_in_11q	11q25
206968_s_at	<i>NFRKB</i>	nuclear factor related to kappaB binding protein	-0,34033	0,006665	downReg_in_11q	11q24.3
208702_x_at	<i>APLP2</i>	amyloid beta (A4) precursor-like protein 2	-0,69365	0,007253	downReg_in_11q	11q24
219515_at	<i>PRDM10</i>	PR domain containing 10	-1,13288	0,013345	downReg_in_11q	11q25
214875_x_at	<i>APLP2</i>	amyloid beta (A4) precursor-like protein 2	-0,67563	0,013626	downReg_in_11q	11q24
211404_s_at	<i>APLP2</i>	amyloid beta (A4) precursor-like protein 2	-0,61154	0,020152	downReg_in_11q	11q24
202005_at	<i>ST14</i>	suppression of tumorigenicity 14 (colon carcinoma)	-0,52252	0,029694	downReg_in_11q	11q24.3
202358_s_at	<i>SNX19</i>	sorting nexin 19	-0,21391	0,047999	downReg_in_11q	11q25
Differentially expressed genes at 11q between cases with 11q-gain/loss pattern and <i>IG-MYC</i> BL						
affy_hg_u133a	symbol	description	logFC	adj.P.Val	gene expression status	Chr Band
204912_at	<i>IL10RA</i>	interleukin 10 receptor, alpha	1,678075	5,51E-09	upReg_in_11q	11q23
213343_s_at	<i>GDPD5</i>	glycerophosphodiester phosphodiesterase domain containing 5	0,688361	1,23E-07	upReg_in_11q	11q13.4
217841_s_at	<i>PPME1</i>	protein phosphatase methylesterase 1	0,444862	2,24E-07	upReg_in_11q	11q13.4
202038_at	<i>UBE4A</i>	ubiquitination factor E4A (UFD2 homolog, yeast)	0,797761	7,37E-07	upReg_in_11q	11q23.3
212906_at	<i>GRAMD1B</i>	GRAM domain containing 1B	0,506668	8,24E-07	upReg_in_11q	11q24.1
32502_at	<i>GDPD5</i>	glycerophosphodiester phosphodiesterase domain containing 5	0,765595	9,07E-07	upReg_in_11q	11q13.4
200054_at	<i>ZNF259</i>	zinc finger protein 259	0,527004	6,01E-06	upReg_in_11q	11q23.3
217958_at	<i>TRAPPC4</i>	trafficking protein particle complex 4	0,890066	6,23E-06	upReg_in_11q	11q23.3
201059_at	<i>CTTN</i>	cortactin	0,736431	1,01E-05	upReg_in_11q	11q13
204236_at	<i>FLI1</i>	Friend leukemia virus integration 1	-0,94562	1,12E-05	downReg_in_11q	11q24.3
49077_at	<i>PPME1</i>	protein phosphatase methylesterase 1	0,325646	1,28E-05	upReg_in_11q	11q13.4
201176_s_at	<i>ARCN1</i>	archain 1	0,841908	1,37E-05	upReg_in_11q	11q23.3
214073_at	<i>CTTN</i>	cortactin	0,366337	1,37E-05	upReg_in_11q	11q13
214369_s_at	<i>RASGRP2</i>	RAS guanyl releasing protein 2 (calcium and DAG-regulated)	-1,0788	2,11E-05	downReg_in_11q	11q13
218531_at	<i>TMEM134</i>	transmembrane protein 134	0,605611	2,88E-05	upReg_in_11q	11q13.2
214724_at	<i>DIXDC1</i>	DIX domain containing 1	0,673977	3,41E-05	upReg_in_11q	11q23.1
219304_s_at	<i>PDGFD</i>	platelet derived growth factor D	1,115638	3,58E-05	upReg_in_11q	11q22.3
210160_at	<i>PAFAH1B2</i>	platelet-activating factor acetylhydrolase 1b, catalytic subunit 2 (30kDa)	0,356262	3,77E-05	upReg_in_11q	11q23
217959_s_at	<i>TRAPPC4</i>	trafficking protein particle complex 4	0,807668	5,56E-05	upReg_in_11q	11q23.3
207213_s_at	<i>USP2</i>	ubiquitin specific peptidase 2	1,013707	5,71E-05	upReg_in_11q	11q23.3
209572_s_at	<i>EED</i>	embryonic ectoderm development	0,810704	6,09E-05	upReg_in_11q	11q14.2

208206_s_at	<i>RASGRP2</i>	RAS guanyl releasing protein 2 (calcium and DAG-regulated)	-0,93394	8,07E-05	downReg_in_11q	11q13
208703_s_at	<i>APLP2</i>	amyloid beta (A4) precursor-like protein 2	-0,99233	8,07E-05	downReg_in_11q	11q24
207573_x_at	<i>ATP5L</i>	ATP synthase, H+ transporting, mitochondrial Fo complex, subunit G	0,667454	9,35E-05	upReg_in_11q	11q23.3
208248_x_at	<i>APLP2</i>	amyloid beta (A4) precursor-like protein 2	-0,85109	9,35E-05	downReg_in_11q	11q24
208704_x_at	<i>APLP2</i>	amyloid beta (A4) precursor-like protein 2	-0,80842	9,35E-05	downReg_in_11q	11q24
218774_at	<i>DCPS</i>	decapping enzyme, scavenger	-0,65704	9,35E-05	downReg_in_11q	11q24.2
208746_x_at	<i>ATP5L</i>	ATP synthase, H+ transporting, mitochondrial Fo complex, subunit G	0,681039	0,00024	upReg_in_11q	11q23.3
209509_s_at	<i>DPAGT1</i>	dolichyl-phosphate (UDP-N-acetylglucosamine) N-acetylglucosaminephosphotransferase 1 (GlcNAc-1-P transferase)	0,505537	0,00024	upReg_in_11q	11q23.3
210453_x_at	<i>ATP5L</i>	ATP synthase, H+ transporting, mitochondrial Fo complex, subunit G	0,661902	0,000444	upReg_in_11q	11q23.3
218491_s_at	<i>THYN1</i>	thymocyte nuclear protein 1	-0,62595	0,000474	downReg_in_11q	11q25
222209_s_at	<i>TMEM135</i>	transmembrane protein 135	1,013816	0,000502	upReg_in_11q	11q14.2
203494_s_at	<i>CEP57</i>	centrosomal protein 57kDa	0,531437	0,000558	upReg_in_11q	11q21
209798_at	<i>NPAT</i>	nuclear protein, ataxia-telangiectasia locus	0,495181	0,000813	upReg_in_11q	11q22.3
221669_s_at	<i>ACAD8</i>	acyl-CoA dehydrogenase family, member 8	-0,49925	0,001474	downReg_in_11q	11q25
212789_at	<i>NCAPD3</i>	non-SMC condensin II complex, subunit D3	-0,51814	0,001519	downReg_in_11q	11q25
213028_at	<i>NFRKB</i>	nuclear factor related to kappaB binding protein	-0,24125	0,001533	downReg_in_11q	11q24.3
204327_s_at	<i>ZNF202</i>	zinc finger protein 202	-0,35395	0,001587	downReg_in_11q	11q23.3
206530_at	<i>RAB30</i>	RAB30, member RAS oncogene family	0,38094	0,001746	upReg_in_11q	11q14.1
203330_s_at	<i>STX5</i>	syntaxin 5	0,264077	0,001913	upReg_in_11q	11q12.3
219053_s_at	<i>VPS37C</i>	vacuolar protein sorting 37 homolog C (S. cerevisiae)	0,313245	0,0023	upReg_in_11q	11q12.2
210786_s_at	<i>FLI1</i>	Friend leukemia virus integration 1	-0,77575	0,002557	downReg_in_11q	11q24.3
202996_at	<i>POLD4</i>	polymerase (DNA-directed), delta 4	0,798108	0,004118	upReg_in_11q	11q13
209694_at	<i>PTS</i>	6-pyruvoyltetrahydropterin synthase	0,747131	0,004316	upReg_in_11q	11q22.3
212506_at	<i>PICALM</i>	phosphatidylinositol binding clathrin assembly protein	0,415084	0,005442	upReg_in_11q	11q14
204251_s_at	<i>CEP164</i>	centrosomal protein 164kDa	0,307823	0,005803	upReg_in_11q	11q23.3
201494_at	<i>PRCP</i>	prolylcarboxypeptidase (angiotensinase C)	0,467707	0,005821	upReg_in_11q	11q14
202359_s_at	<i>SNX19</i>	sorting nexin 19	-0,27369	0,006075	downReg_in_11q	11q25
212568_s_at	<i>DLAT</i>	dihydrolipoamide S-acetyltransferase	0,653693	0,006245	upReg_in_11q	11q23.1
216905_s_at	<i>ST14</i>	suppression of tumorigenicity 14 (colon carcinoma)	-0,66041	0,006449	downReg_in_11q	11q24.3
206968_s_at	<i>NFRKB</i>	nuclear factor related to kappaB binding protein	-0,34033	0,006665	downReg_in_11q	11q24.3
218483_s_at	<i>IFT46</i>	intraflagellar transport 46 homolog (Chlamydomonas)	0,350362	0,006707	upReg_in_11q	11q23.3
203391_at	<i>FKBP2</i>	FK506 binding protein 2, 13kDa	0,335952	0,006804	upReg_in_11q	11q13.1
202076_at	<i>BIRC2</i>	baculoviral IAP repeat containing 2	0,431788	0,007051	upReg_in_11q	11q22
208702_x_at	<i>APLP2</i>	amyloid beta (A4) precursor-like protein 2	-0,69365	0,007253	downReg_in_11q	11q24
34206_at	<i>ARAP1</i>	ArfGAP with RhoGAP domain, ankyrin repeat and PH domain 1	0,317264	0,007366	upReg_in_11q	11q13.4
210538_s_at	<i>BIRC3</i>	baculoviral IAP repeat containing 3	1,110038	0,007493	upReg_in_11q	11q22
216250_s_at	<i>LPXN</i>	leupaxin	0,610693	0,007722	upReg_in_11q	11q12.1
201119_s_at	<i>COX8A</i>	cytochrome c oxidase subunit VIIIA (ubiquitous)	0,445603	0,008009	upReg_in_11q	11q13.1
203491_s_at	<i>CEP57</i>	centrosomal protein 57kDa	0,518688	0,008215	upReg_in_11q	11q21
1861_at	<i>BAD</i>	BCL2-associated agonist of cell death	0,282945	0,008511	upReg_in_11q	11q13.1
204757_s_at	<i>C2CD2L</i>	C2CD2-like	0,216491	0,01	upReg_in_11q	11q23.3
216615_s_at	<i>HTR3A</i>	5-hydroxytryptamine (serotonin) receptor 3A	0,351571	0,010081	upReg_in_11q	11q23.1
218357_s_at	<i>TIMM8B</i>	translocase of inner mitochondrial membrane 8 homolog B (yeast)	0,579248	0,010347	upReg_in_11q	11q23.1
213149_at	<i>DLAT</i>	dihydrolipoamide S-acetyltransferase	0,555759	0,010535	upReg_in_11q	11q23.1
219515_at	<i>PRDM10</i>	PR domain containing 10	-1,13288	0,013345	downReg_in_11q	11q25
204329_s_at	<i>ZNF202</i>	zinc finger protein 202	-0,1852	0,013414	downReg_in_11q	11q23.3
214211_at	<i>FTH1</i>	ferritin, heavy polypeptide 1	0,598449	0,013606	upReg_in_11q	11q13
214875_x_at	<i>APLP2</i>	amyloid beta (A4) precursor-like protein 2	-0,67563	0,013626	downReg_in_11q	11q24
205395_s_at	<i>MRE11A</i>	MRE11 meiotic recombination 11 homolog A (S. cerevisiae)	0,380975	0,014142	upReg_in_11q	11q21

203252_at	<i>CDK2AP2</i>	cyclin-dependent kinase 2 associated protein 2	0,578801	0,014145	upReg_in_11q	11q13
209364_at	<i>BAD</i>	BCL2-associated agonist of cell death	0,299575	0,014521	upReg_in_11q	11q13.1
203620_s_at	<i>FCHSD2</i>	FCH and double SH3 domains 2	-0,5122	0,014803	downReg_in_11q	11q13.4
208289_s_at	<i>EI24</i>	etoposide induced 2.4 mRNA	-0,3896	0,015367	downReg_in_11q	11q24
218314_s_at	<i>C11orf57</i>	chromosome 11 open reading frame 57	0,288811	0,015399	upReg_in_11q	11q23.1
220964_s_at	<i>RAB1B</i>	RAB1B, member RAS oncogene family myeloid/lymphoid or mixed-lineage leukemia (trithorax homolog, Drosophila)	0,265311	0,015707	upReg_in_11q	11q12
212080_at	<i>MLL</i>		0,440896	0,015933	upReg_in_11q	11q23
209428_s_at	<i>ZFPL1</i>	zinc finger protein-like 1	0,189295	0,017234	upReg_in_11q	11q13
219806_s_at	<i>C11orf75</i>	chromosome 11 open reading frame 75	0,644553	0,017642	upReg_in_11q	11q21
200748_s_at	<i>FTH1</i>	ferritin, heavy polypeptide 1	0,565409	0,017656	upReg_in_11q	11q13
219021_at	<i>RNF121</i>	ring finger protein 121	0,208214	0,019922	upReg_in_11q	11q13.4
211404_s_at	<i>APLP2</i>	amyloid beta (A4) precursor-like protein 2	-0,61154	0,020152	downReg_in_11q	11q24
208745_at	<i>ATP5L</i>	ATP synthase, H+ transporting, mitochondrial Fo complex, subunit G	0,452209	0,020371	upReg_in_11q	11q23.3
217418_x_at	<i>MS4A1</i>	membrane-spanning 4-domains, subfamily A, member 1	-0,9361	0,022052	downReg_in_11q	11q12
210356_x_at	<i>MS4A1</i>	membrane-spanning 4-domains, subfamily A, member 1	-0,94168	0,022471	downReg_in_11q	11q12
220934_s_at	<i>TMEM223</i>	transmembrane protein 223	0,325398	0,024934	upReg_in_11q	11q12.3
214657_s_at	<i>NEAT1</i>	nuclear paraspeckle assembly transcript 1 (non-protein coding)	0,383265	0,02784	upReg_in_11q	11q13.1
200846_s_at	<i>PPP1CA</i>	protein phosphatase 1, catalytic subunit, alpha isozyme	0,428579	0,0292	upReg_in_11q	11q13
202005_at	<i>ST14</i>	suppression of tumorigenicity 14 (colon carcinoma)	-0,52252	0,029694	downReg_in_11q	11q24.3
210656_at	<i>EED</i>	embryonic ectoderm development	0,450205	0,029694	upReg_in_11q	11q14.2
203040_s_at	<i>HMBS</i>	hydroxymethylbilane synthase	0,395019	0,030187	upReg_in_11q	11q23.3
212516_at	<i>ARAP1</i>	ArfGAP with RhoGAP domain, ankyrin repeat and PH domain 1	0,275375	0,030918	upReg_in_11q	11q13.4
214251_s_at	<i>NUMA1</i>	nuclear mitotic apparatus protein 1	-0,6312	0,032008	downReg_in_11q	11q13
56256_at	<i>SIDT2</i>	SID1 transmembrane family, member 2	0,507588	0,034517	upReg_in_11q	11q23.3
214074_s_at	<i>CTTN</i>	cortactin	0,177746	0,03607	upReg_in_11q	11q13
203532_x_at	<i>CUL5</i>	cullin 5	0,235816	0,036078	upReg_in_11q	11q22.3
205436_s_at	<i>H2AFX</i>	H2A histone family, member X	0,54258	0,037799	upReg_in_11q	11q23.3
217002_s_at	<i>HTR3A</i>	5-hydroxytryptamine (serotonin) receptor 3A leucine rich repeat and fibronectin type III domain containing 4	0,275376	0,037823	upReg_in_11q	11q23.1
219491_at	<i>LRFN4</i>		-0,60122	0,03893	downReg_in_11q	11q13.2
211150_s_at	<i>DLAT</i>	dihydrolipoamide S-acetyltransferase	0,568386	0,040695	upReg_in_11q	11q23.1
218765_at	<i>SIDT2</i>	SID1 transmembrane family, member 2	0,285941	0,040985	upReg_in_11q	11q23.3
216624_s_at	<i>MLL</i>	myeloid/lymphoid or mixed-lineage leukemia (trithorax homolog, Drosophila)	0,238159	0,043089	upReg_in_11q	11q23
202358_s_at	<i>SNX19</i>	sorting nexin 19	-0,21391	0,047999	downReg_in_11q	11q25
209581_at	<i>PLA2G16</i>	phospholipase A2, group XVI	0,371652	0,049396	upReg_in_11q	11q12.3
217774_s_at	<i>TRMT112</i>	tRNA methyltransferase 11-2 homolog (S. cerevisiae)	0,364092	0,049559	upReg_in_11q	11q13.1
204164_at	<i>SIPA1</i>	signal-induced proliferation-associated 1	0,357053	0,049819	upReg_in_11q	11q13

logFC: log fold change; adj.P.Val: adjusted p-value; downReg: downregulated; upReg: upregulated

Supplemental Table 8. Differentially expressed genes between cases with 11q-gain/loss pattern(cohort 3) (n=6) and DLBCL (n=198)

Differentially expressed genes in the 11q minimal region of gain between cases with 11q-gain/loss pattern and DLBCL						
affy_hg_u133a	symbol	description	logFC	adj.P.Val	gene expression status	Chr Band
210160_at	<i>PAFAH1B2</i>	platelet-activating factor acetylhydrolase 1b, catalytic subunit 2 (30kDa)	0,3549459	3,47E-05	upReg_in_11q	11q23
200054_at	<i>ZNF259</i>	zinc finger protein 259	0,6010693	6,65E-05	upReg_in_11q	11q23.3
204251_s_at	<i>CEP164</i>	centrosomal protein 164kDa	0,3548958	0,0001943	upReg_in_11q	11q23.3
Differentially expressed genes in the 11q minimal region of loss between cases with 11q-gain/loss pattern and DLBCL						
affy_hg_u133a	symbol	description	logFC	adj.P.Val	gene expression status	Chr Band
221669_s_at	<i>ACAD8</i>	acyl-CoA dehydrogenase family, member 8	-0,602787	4,07E-05	downReg_in_11q	11q25
204236_at	<i>FLI1</i>	Friend leukemia virus integration 1	-0,942324	0,0007944	downReg_in_11q	11q24.3
219515_at	<i>PRDM10</i>	PR domain containing 10	0,4111526	0,0031113	upReg_in_11q	11q25
218491_s_at	<i>THYN1</i>	thymocyte nuclear protein 1	-0,584312	0,0062082	downReg_in_11q	11q25
202359_s_at	<i>SNX19</i>	sorting nexin 19	-0,319848	0,0116245	downReg_in_11q	11q25
202358_s_at	<i>SNX19</i>	sorting nexin 19	-0,277251	0,0117535	downReg_in_11q	11q25
210786_s_at	<i>FLI1</i>	Friend leukemia virus integration 1	-0,689029	0,0150662	downReg_in_11q	11q24.3
220677_s_at	<i>ADAMTS8</i>	ADAM metalloproteinase with thrombospondin type 1 motif, 8	-0,152753	0,0494953	downReg_in_11q	11q25
Differentially expressed genes at 11q between cases with 11q-gain/loss pattern and DLBCL						
affy_hg_u133a	symbol	description	logFC	adj.P.Val	gene expression status	Chr Band
207213_s_at	<i>USP2</i>	ubiquitin specific peptidase 2	0,9782071	1,75E-12	upReg_in_11q	11q23.3
205412_at	<i>ACAT1</i>	acetyl-CoA acetyltransferase 1	1,2478204	3,53E-09	upReg_in_11q	11q22.3
207573_x_at	<i>ATP5L</i>	ATP synthase, H+ transporting, mitochondrial Fo complex, subunit G	0,9815732	5,59E-09	upReg_in_11q	11q23.3
208746_x_at	<i>ATP5L</i>	ATP synthase, H+ transporting, mitochondrial Fo complex, subunit G	1,0297151	1,05E-08	upReg_in_11q	11q23.3
210453_x_at	<i>ATP5L</i>	ATP synthase, H+ transporting, mitochondrial Fo complex, subunit G	0,9972158	1,37E-08	upReg_in_11q	11q23.3
203040_s_at	<i>HMBS</i>	hydroxymethylbilane synthase	0,8000295	5,95E-08	upReg_in_11q	11q23.3
204266_s_at	<i>CHKA</i>	choline kinase alpha	0,6064674	1,40E-07	upReg_in_11q	11q13.2
218281_at	<i>MRPL48</i>	mitochondrial ribosomal protein L48	0,7914415	2,57E-06	upReg_in_11q	11q13.4
222209_s_at	<i>TMEM135</i>	transmembrane protein 135	0,9954209	5,62E-06	upReg_in_11q	11q14.2
209310_s_at	<i>CASP4</i>	caspase 4, apoptosis-related cysteine peptidase	-0,900248	1,12E-05	downReg_in_11q	11q22.3
208745_at	<i>ATP5L</i>	ATP synthase, H+ transporting, mitochondrial Fo complex, subunit G	0,737387	1,21E-05	upReg_in_11q	11q23.3
211150_s_at	<i>DLAT</i>	dihydrolipoamide S-acetyltransferase	0,94146	1,25E-05	upReg_in_11q	11q23.1
218314_s_at	<i>C11orf57</i>	chromosome 11 open reading frame 57	0,5146329	1,55E-05	upReg_in_11q	11q23.1
218483_s_at	<i>IFT46</i>	intraflagellar transport 46 homolog (Chlamydomonas)	0,4791343	2,62E-05	upReg_in_11q	11q23.3
205449_at	<i>SAC3D1</i>	SAC3 domain containing 1	0,9570918	3,06E-05	upReg_in_11q	11q13.1
218357_s_at	<i>TIMM8B</i>	translocase of inner mitochondrial membrane 8 homolog B (yeast)	0,8751176	3,07E-05	upReg_in_11q	11q23.1
210160_at	<i>PAFAH1B2</i>	platelet-activating factor acetylhydrolase 1b, catalytic subunit 2 (30kDa)	0,3549459	3,47E-05	upReg_in_11q	11q23
221669_s_at	<i>ACAD8</i>	acyl-CoA dehydrogenase family, member 8	-0,602787	4,07E-05	downReg_in_11q	11q25
200054_at	<i>ZNF259</i>	zinc finger protein 259	0,6010693	6,65E-05	upReg_in_11q	11q23.3
209694_at	<i>PTS</i>	6-pyruvoyltetrahydropterin synthase	0,9481615	7,58E-05	upReg_in_11q	11q22.3
212568_s_at	<i>DLAT</i>	dihydrolipoamide S-acetyltransferase	0,9515238	0,0001165	upReg_in_11q	11q23.1
217958_at	<i>TRAPPC4</i>	trafficking protein particle complex 4	0,7829267	0,0001208	upReg_in_11q	11q23.3
204251_s_at	<i>CEP164</i>	centrosomal protein 164kDa	0,3548958	0,0001943	upReg_in_11q	11q23.3
220934_s_at	<i>TMEM223</i>	transmembrane protein 223	0,429785	0,0003356	upReg_in_11q	11q12.3
204441_s_at	<i>POLA2</i>	polymerase (DNA directed), alpha 2 (70kD subunit)	0,5943025	0,0003477	upReg_in_11q	11q13.1
204233_s_at	<i>CHKA</i>	choline kinase alpha	0,5190812	0,0003966	upReg_in_11q	11q13.2
214724_at	<i>DIXDC1</i>	DIX domain containing 1	0,5618571	0,0003994	upReg_in_11q	11q23.1
202038_at	<i>UBE4A</i>	ubiquitination factor E4A (UFD2 homolog, yeast)	0,6837696	0,0005622	upReg_in_11q	11q23.3

213149_at	<i>DLAT</i>	dihydrolipoamide S-acetyltransferase tRNA methyltransferase 11-2 homolog (S. cerevisiae)	0,7956132	0,0007382	upReg_in_11q	11q23.1
217774_s_at	<i>TRMT112</i>		0,662946	0,0007466	upReg_in_11q	11q13.1
204236_at	<i>FLI1</i>	Friend leukemia virus integration 1	-0,942324	0,0007944	downReg_in_11q	11q24.3
202170_s_at	<i>AASDHPPT</i>	aminoadipate-semialdehyde dehydrogenase-phosphopantetheinyl transferase	0,6202666	0,0008132	upReg_in_11q	11q22
203103_s_at	<i>PRPF19</i>	PRP19/PSO4 pre-mRNA processing factor 19 homolog (S. cerevisiae)	0,5934282	0,0009286	upReg_in_11q	11q12.2
217866_at	<i>CPSF7</i>	cleavage and polyadenylation specific factor 7, 59kDa	0,4739024	0,0009613	upReg_in_11q	11q12.2
200957_s_at	<i>SSRP1</i>	structure specific recognition protein 1	0,6256101	0,0011505	upReg_in_11q	11q12
201119_s_at	<i>COX8A</i>	cytochrome c oxidase subunit VIIIa (ubiquitous)	0,554285	0,001162	upReg_in_11q	11q13.1
217841_s_at	<i>PPME1</i>	protein phosphatase methylesterase 1	0,3831073	0,0012401	upReg_in_11q	11q13.4
202306_at	<i>POLR2G</i>	polymerase (RNA) II (DNA directed) polypeptide G	0,6241404	0,0012498	upReg_in_11q	11q13.1
204218_at	<i>C11orf51</i>	chromosome 11 open reading frame 51	0,4460535	0,0012687	upReg_in_11q	11q13.4
221712_s_at	<i>WDR74</i>	WD repeat domain 74	0,4779026	0,0012687	upReg_in_11q	11q12.3
213330_s_at	<i>STIP1</i>	stress-induced-phosphoprotein 1	0,6279378	0,0014284	upReg_in_11q	11q13
219769_at	<i>INCENP</i>	inner centromere protein antigens 135/155kDa	0,3002023	0,001461	upReg_in_11q	11q12.3
212076_at	<i>MLL</i>	myeloid/lymphoid or mixed-lineage leukemia (trithorax homolog, Drosophila)	0,4436059	0,0018087	upReg_in_11q	11q23
205395_s_at	<i>MRE11A</i>	MRE11 meiotic recombination 11 homolog A (S. cerevisiae)	0,6067197	0,0018587	upReg_in_11q	11q21
217959_s_at	<i>TRAPPC4</i>	trafficking protein particle complex 4	0,6957569	0,0021022	upReg_in_11q	11q23.3
210356_x_at	<i>MS4A1</i>	membrane-spanning 4-domains, subfamily A, member 1	-1,288255	0,0021938	downReg_in_11q	11q12
217418_x_at	<i>MS4A1</i>	membrane-spanning 4-domains, subfamily A, member 1	-1,264078	0,0023069	downReg_in_11q	11q12
202065_s_at	<i>PPFIA1</i>	protein tyrosine phosphatase, receptor type, f polypeptide (PTPRF), interacting protein (liprin), alpha 1	0,2399142	0,0023772	upReg_in_11q	11q13.3
209032_s_at	<i>CADM1</i>	cell adhesion molecule 1	0,7988333	0,0026265	upReg_in_11q	11q23.2
49077_at	<i>PPME1</i>	protein phosphatase methylesterase 1	0,3329125	0,002796	upReg_in_11q	11q13.4
204757_s_at	<i>C2CD2L</i>	C2CD2-like	0,2190684	0,0028128	upReg_in_11q	11q23.3
204767_s_at	<i>FEN1</i>	flap structure-specific endonuclease 1	0,7986502	0,0028455	upReg_in_11q	11q12
219515_at	<i>PRDM10</i>	PR domain containing 10	0,4111526	0,0031113	upReg_in_11q	11q25
201176_s_at	<i>ARCN1</i>	archain 1	0,5765224	0,0033718	upReg_in_11q	11q23.3
218734_at	<i>NAA40</i>	N(alpha)-acetyltransferase 40, NatD catalytic subunit, homolog (S. cerevisiae)	0,365137	0,0040586	upReg_in_11q	11q13.1
200918_s_at	<i>SRPR</i>	signal recognition particle receptor (docking protein)	-0,557199	0,004249	downReg_in_11q	11q24.2
212080_at	<i>MLL</i>	myeloid/lymphoid or mixed-lineage leukemia (trithorax homolog, Drosophila)	0,456507	0,004249	upReg_in_11q	11q23
219162_s_at	<i>MRPL11</i>	mitochondrial ribosomal protein L11	0,5186287	0,0042961	upReg_in_11q	11q13.3
211986_at	<i>AHNAK</i>	AHNAK nucleoprotein	-0,910851	0,0043516	downReg_in_11q	11q12.2
212397_at	<i>RDX</i>	radixin	-0,886068	0,0043808	downReg_in_11q	11q23
205436_s_at	<i>H2AFX</i>	H2A histone family, member X	0,8504199	0,0044803	upReg_in_11q	11q23.3
208619_at	<i>DDB1</i>	damage-specific DNA binding protein 1, 127kDa	0,4281291	0,0047419	upReg_in_11q	11q12.2
209798_at	<i>NPAT</i>	nuclear protein, ataxia-telangiectasia locus protein tyrosine phosphatase, receptor type, f polypeptide (PTPRF), interacting protein (liprin), alpha 1	0,4925735	0,0049464	upReg_in_11q	11q22.3
210236_at	<i>PPFIA1</i>		0,278476	0,0053127	upReg_in_11q	11q13.3
203491_s_at	<i>CEP57</i>	centrosomal protein 57kDa	0,6608241	0,0059996	upReg_in_11q	11q21
218491_s_at	<i>THYN1</i>	thymocyte nuclear protein 1	-0,584312	0,0062082	downReg_in_11q	11q25
217980_s_at	<i>MRPL16</i>	mitochondrial ribosomal protein L16	0,4996882	0,0062715	upReg_in_11q	11q12.1
216624_s_at	<i>MLL</i>	myeloid/lymphoid or mixed-lineage leukemia (trithorax homolog, Drosophila)	0,2662181	0,0069172	upReg_in_11q	11q23
218774_at	<i>DCPS</i>	decapping enzyme, scavenger	-0,509863	0,0071109	downReg_in_11q	11q24.2
204768_s_at	<i>FEN1</i>	flap structure-specific endonuclease 1	0,7525314	0,0077506	upReg_in_11q	11q12
221818_at	<i>INTS5</i>	integrator complex subunit 5	0,295263	0,0084659	upReg_in_11q	11q12.3
221580_s_at	<i>TAF1D</i>	TATA box binding protein (TBP)-associated factor, RNA polymerase I, D, 41kDa	0,6899697	0,0085511	upReg_in_11q	11q21
202645_s_at	<i>MEN1</i>	multiple endocrine neoplasia I	0,439182	0,0086418	upReg_in_11q	11q13

220613_s_at	<i>SYTL2</i>	synaptotagmin-like 2	0,2965953	0,0091833	upReg_in_11q	11q14
204812_at	<i>ZW10</i>	ZW10, kinetochore associated, homolog (Drosophila)	0,294103	0,0094026	upReg_in_11q	11q23.2
204977_at	<i>DDX10</i>	DEAD (Asp-Glu-Ala-Asp) box polypeptide 10	0,455369	0,0097333	upReg_in_11q	11q22.3
212525_s_at	<i>H2AFX</i>	H2A histone family, member X	0,5503475	0,0100177	upReg_in_11q	11q23.3
200956_s_at	<i>SSRP1</i>	structure specific recognition protein 1	0,6316079	0,0109471	upReg_in_11q	11q12
220998_s_at	<i>UNC93B1</i>	unc-93 homolog B1 (C. elegans)	-0,340523	0,0110751	downReg_in_11q	11q13
202359_s_at	<i>SNX19</i>	sorting nexin 19	-0,319848	0,0116245	downReg_in_11q	11q25
202358_s_at	<i>SNX19</i>	sorting nexin 19	-0,277251	0,0117535	downReg_in_11q	11q25
202883_s_at	<i>PPP2R1B</i>	protein phosphatase 2, regulatory subunit A, beta	0,5078317	0,0122387	upReg_in_11q	11q23.2
212680_x_at	<i>PPP1R14B</i>	protein phosphatase 1, regulatory (inhibitor) subunit 14B	0,6687539	0,0129027	upReg_in_11q	11q13
222369_at	<i>NAA40</i>	N(alpha)-acetyltransferase 40, NatD catalytic subunit, homolog (S. cerevisiae)	0,5182417	0,0135619	upReg_in_11q	11q13.1
203494_s_at	<i>CEP57</i>	centrosomal protein 57kDa	0,4972319	0,0137427	upReg_in_11q	11q21
203190_at	<i>NDUFS8</i>	NADH dehydrogenase (ubiquinone) Fe-S protein 8, 23kDa (NADH-coenzyme Q reductase)	0,5311954	0,0139541	upReg_in_11q	11q13
204828_at	<i>RAD9A</i>	RAD9 homolog A (S. pombe)	0,2119539	0,0141123	upReg_in_11q	11q13.2
53968_at	<i>INTS5</i>	integrator complex subunit 5	0,3620342	0,014615	upReg_in_11q	11q12.3
210786_s_at	<i>FLI1</i>	Friend leukemia virus integration 1	-0,689029	0,0150662	downReg_in_11q	11q24.3
209572_s_at	<i>EED</i>	embryonic ectoderm development	0,701465	0,0153376	upReg_in_11q	11q14.2
211042_x_at	<i>MCAM</i>	melanoma cell adhesion molecule	0,4593377	0,0160341	upReg_in_11q	11q23.3
202886_s_at	<i>PPP2R1B</i>	protein phosphatase 2, regulatory subunit A, beta	0,5394457	0,01658	upReg_in_11q	11q23.2
214074_s_at	<i>CTTN</i>	cortactin	0,1667822	0,0166839	upReg_in_11q	11q13
203119_at	<i>CCDC86</i>	coiled-coil domain containing 86	0,4950085	0,0189621	upReg_in_11q	11q12.2
218906_x_at	<i>KLC2</i>	kinesin light chain 2	0,2888295	0,0195307	upReg_in_11q	11q13.2
218566_s_at	<i>CHORDC1</i>	cysteine and histidine-rich domain (CHORD) containing 1	0,6585327	0,0203891	upReg_in_11q	11q14.3
208714_at	<i>NDUFV1</i>	NADH dehydrogenase (ubiquinone) flavoprotein 1, 51kDa	0,4862397	0,0210139	upReg_in_11q	11q13
200846_s_at	<i>PPP1CA</i>	protein phosphatase 1, catalytic subunit, alpha isozyyme	0,4665403	0,0217548	upReg_in_11q	11q13
209970_x_at	<i>CASP1</i>	caspase 1, apoptosis-related cysteine peptidase (interleukin 1, beta, convertase)	-0,741733	0,0218502	downReg_in_11q	11q23
204178_s_at	<i>RBM14</i>	RNA binding motif protein 14	0,405609	0,0230713	upReg_in_11q	11q13.2
205267_at	<i>POU2AF1</i>	POU class 2 associating factor 1	0,8399652	0,0236727	upReg_in_11q	11q23.1
208712_at	<i>CCND1</i>	cyclin D1	-0,498926	0,0241934	downReg_in_11q	11q13
212078_s_at	<i>MLL</i>	myeloid/lymphoid or mixed-lineage leukemia (trithorax homolog, Drosophila)	0,2568695	0,0251639	upReg_in_11q	11q23
209892_at	<i>FUT4</i>	fucosyltransferase 4 (alpha (1,3) fucosyltransferase, myeloid-specific)	-0,370716	0,0263634	downReg_in_11q	11q21
32502_at	<i>GDPD5</i>	glycerophosphodiester phosphodiesterase domain containing 5	0,5406836	0,0268002	upReg_in_11q	11q13.4
210125_s_at	<i>BANF1</i>	barrier to autointegration factor 1	0,5516835	0,0271706	upReg_in_11q	11q13.1
212573_at	<i>ENDOD1</i>	endonuclease domain containing 1	0,4988896	0,0290231	upReg_in_11q	11q21
204969_s_at	<i>RDX</i>	radixin	-0,384763	0,0295712	downReg_in_11q	11q23
203189_s_at	<i>NDUFS8</i>	NADH dehydrogenase (ubiquinone) Fe-S protein 8, 23kDa (NADH-coenzyme Q reductase)	0,4661644	0,0300055	upReg_in_11q	11q13
218531_at	<i>TMEM134</i>	transmembrane protein 134	0,4318852	0,0303758	upReg_in_11q	11q13.2
211367_s_at	<i>CASP1</i>	caspase 1, apoptosis-related cysteine peptidase (interleukin 1, beta, convertase)	-0,806784	0,0312463	downReg_in_11q	11q23
218194_at	<i>REXO2</i>	REX2, RNA exonuclease 2 homolog (S. cerevisiae)	0,5793743	0,0314286	upReg_in_11q	11q23.2
212079_s_at	<i>MLL</i>	myeloid/lymphoid or mixed-lineage leukemia (trithorax homolog, Drosophila)	0,3532438	0,0328347	upReg_in_11q	11q23
203853_s_at	<i>GAB2</i>	GRB2-associated binding protein 2	-0,43939	0,0343981	downReg_in_11q	11q14.1
210235_s_at	<i>PPFIA1</i>	protein tyrosine phosphatase, receptor type, f polypeptide (PTPRF), interacting protein (liprin), alpha 1	0,2600899	0,0344788	upReg_in_11q	11q13.3
206495_s_at	<i>HINFP</i>	histone H4 transcription factor	0,2077073	0,0350076	upReg_in_11q	11q23.3
205011_at	<i>VWA5A</i>	von Willebrand factor A domain containing 5A	-0,284003	0,0358018	downReg_in_11q	11q24.1
214789_x_at	<i>SRSF8</i>	serine/arginine-rich splicing factor 8	0,3094599	0,0361384	upReg_in_11q	11q22
200091_s_at	<i>RPS25</i>	ribosomal protein S25	0,4548306	0,0371266	upReg_in_11q	11q23.3

214073_at	<i>CTTN</i>	cortactin	0,1964462	0,0372901	upReg_in_11q	11q13
200986_at	<i>SERPING1</i>	serpin peptidase inhibitor, clade G (C1 inhibitor), member 1	-1,092758	0,0374944	downReg_in_11q	11q12.1
212398_at	<i>RDX</i>	radixin	-0,538168	0,0380011	downReg_in_11q	11q23
200019_s_at	<i>FAU</i>	Finkel-Biskis-Reilly murine sarcoma virus (FBR-MuSV) ubiquitously expressed	0,4888132	0,0381046	upReg_in_11q	11q13
206011_at	<i>CASP1</i>	caspace 1, apoptosis-related cysteine peptidase (interleukin 1, beta, convertase)	-0,586665	0,0408942	downReg_in_11q	11q23
49111_at	<i>ARRB1</i>	arrestin, beta 1	-0,213388	0,0408942	downReg_in_11q	11q13
209862_s_at	<i>CEP57</i>	centrosomal protein 57kDa	0,4338938	0,0411261	upReg_in_11q	11q21
202978_s_at	<i>CREBZF</i>	CREB/ATF bZIP transcription factor phosphatidylinositol binding clathrin assembly protein	0,391999	0,042303	upReg_in_11q	11q14
203134_at	<i>PICALM</i>	protein	0,2562355	0,0423501	upReg_in_11q	11q14
210102_at	<i>VWA5A</i>	von Willebrand factor A domain containing 5A translocase of inner mitochondrial membrane 10 homolog (yeast)	-0,28035	0,0423501	downReg_in_11q	11q24.1
218408_at	<i>TIMM10</i>	homolog (yeast)	0,4226004	0,0445603	upReg_in_11q	11q12.1
200619_at	<i>SF3B2</i>	splicing factor 3b, subunit 2, 145kDa	0,331762	0,044694	upReg_in_11q	11q13.1
209030_s_at	<i>CADM1</i>	cell adhesion molecule 1	0,924763	0,0455815	upReg_in_11q	11q23.2
221277_s_at	<i>PUS3</i>	pseudouridylate synthase 3	-0,285858	0,0466813	downReg_in_11q	11q24.2
221637_s_at	<i>C11orf48</i>	chromosome 11 open reading frame 48	0,4580805	0,0469024	upReg_in_11q	11q12.3
211366_x_at	<i>CASP1</i>	caspace 1, apoptosis-related cysteine peptidase (interleukin 1, beta, convertase)	-0,653807	0,0476959	downReg_in_11q	11q23
211368_s_at	<i>CASP1</i>	caspace 1, apoptosis-related cysteine peptidase (interleukin 1, beta, convertase)	-0,750575	0,0482096	downReg_in_11q	11q23
221622_s_at	<i>TMEM126B</i>	transmembrane protein 126B	0,4878169	0,0484394	upReg_in_11q	11q14.1
220677_s_at	<i>ADAMTS8</i>	ADAM metallopeptidase with thrombospondin type 1 motif, 8	-0,152753	0,0494953	downReg_in_11q	11q25
218641_at	<i>C11orf95</i>	chromosome 11 open reading frame 95	0,3267782	0,0499187	upReg_in_11q	11q13

logFC: log fold change; adj.P.Val: adjusted p-value; ; downReg: downregulated; upReg: upregulated

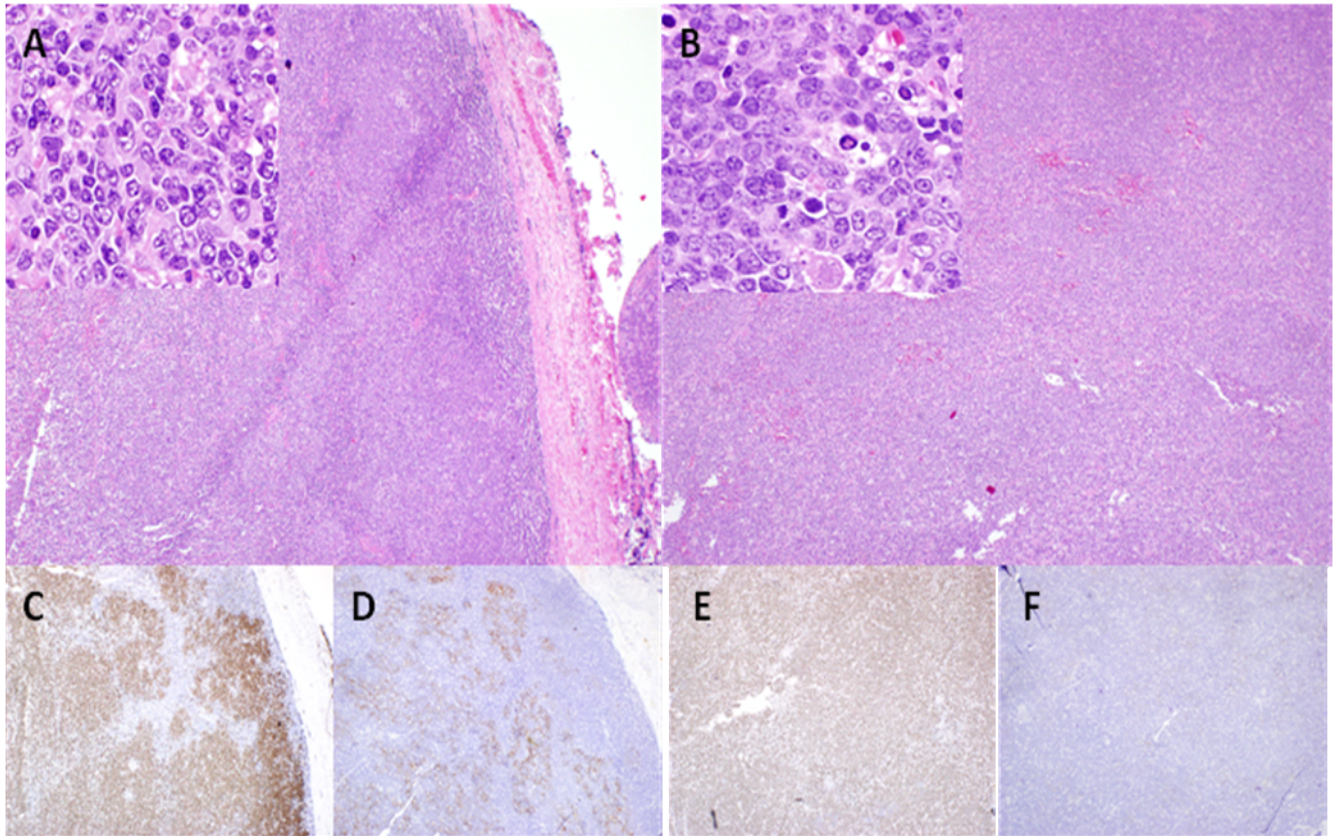
Supplemental Table 9. Mutational study on the *ETS1* gene.

Case	Mutation type	Position*	Ref nt [†]	Obs nt	Predominant allele	Effect [‡]	SIFT prediction (score [¶])	Polyphen prediction
Case 1	unmutated	-	-	-	-	-	-	-
Case 2	unmutated	-	-	-	-	-	-	-
Case 3	splice site	127897017	G	A	mut	-	-	-
Case 4	non-mutated							
Case 5	missense	127897075	C	G	mut	P9A	Tolerated (0.07)	Probably damaging
	silent	127838731	C	T	wt	G331G	-	-
Case 6	unmutated	-	-	-	-	-	-	-
Case 7	missense	127897036	G	A	wt	E22K	Tolerated (0.09)	Benign
	missense	127855487	C	T	balanced	S267F	Tolerated (0.70)	Benign
	silent	127860006	C	T	mut homo	D204D	-	-
Case 8	nonsense	127861193	T	A	mut	Y154X	-	-
Case 9	not applicable#							
Case 10	unmutated	-	-	-	-	-	-	-
Case 11	unmutated	-	-	-	-	-	-	-
Case 12	not done							
MPI-078	unmutated	-	-	-	-	-	-	-
MPI-086	unmutated	-	-	-	-	-	-	-
MPI-148	not done							
MPI-315	unmutated	-	-	-	-	-	-	-
MPI-382	unmutated							
SU-DHL-5	unmutated	-	-	-	-	-	-	-
HT	unmutated	-	-	-	-	-	-	-

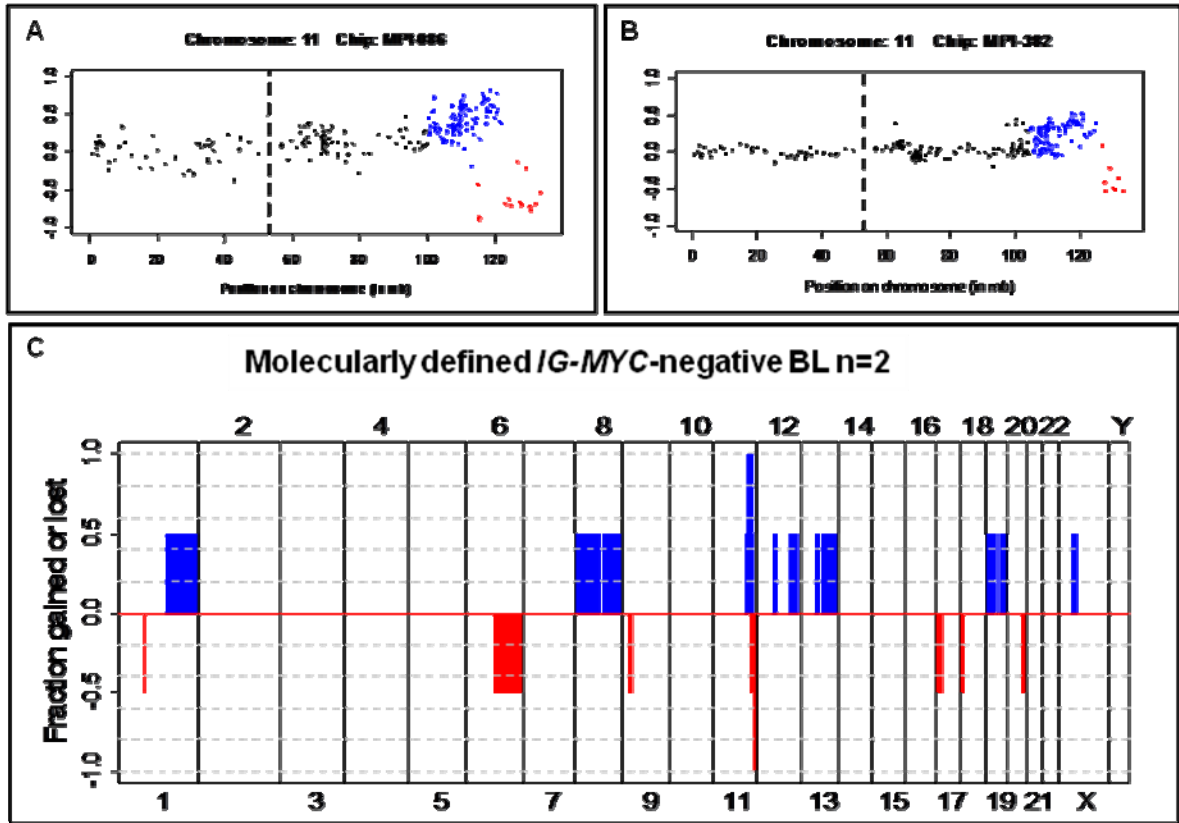
*Numbering according to the Human Genome hg18 assembly; [†]Minus strand; [‡]Numbering according to GenBank accession No. NP_005229.1 (protein); [¶]Threshold for intolerance is 0.05; #Case 9 showed a homozygous deletion including *ETS1* Abbreviations: Ref nt, reference nucleotide; Obs nt, observed nucleotide.

V. Supplemental figures

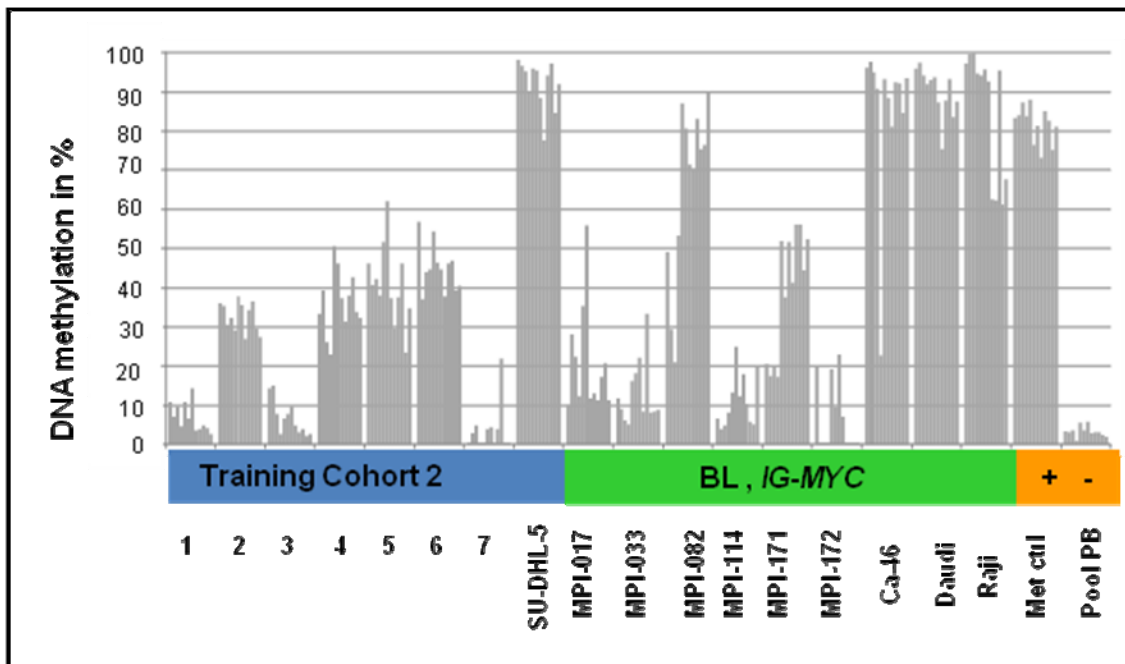
Supplemental Figure 1. Case 10 presented with follicular (A, C, D) and diffuse (B, E, F) growth pattern. This finding including the presence of follicular dendritic cells prompted the pathology panel in the review blinded for molecular analysis to diagnose a follicular lymphoma with transformation to DLBCL. The diffuse areas however, show small blasts with a narrow rim of cytoplasm and a starry sky pattern (B). The proliferation is more than 90% (C+E). (A+B Hematoxylin and Eosin, C+E Ki67, D+F CD21).



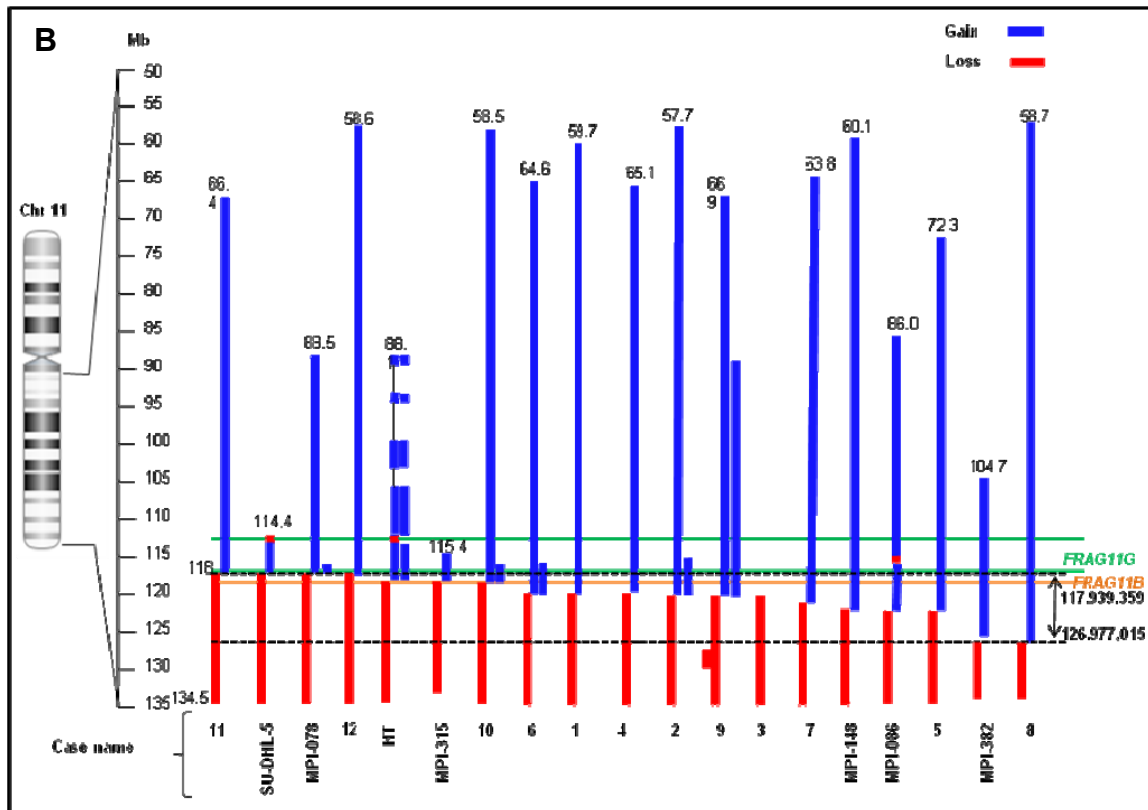
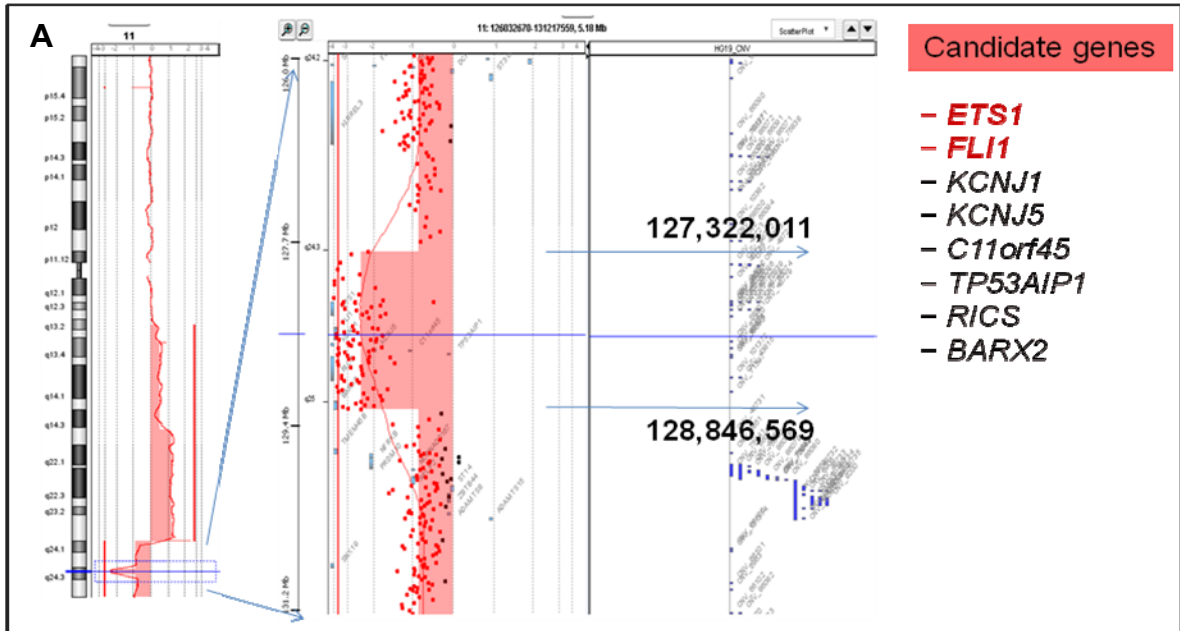
Supplemental Figure 2. 11q alterations in *MYC*-negative lymphomas classified as BL by both gene expression classifiers. Chromosome 11 profile of MMML cases MPI-086 (A) and MPI-382 (B). (C) Proportion of gain and losses along chromosomes of cases MPI-086 and MPI-382. Blue columns indicate chromosomal gain, whereas red columns indicate loss of genetic material.



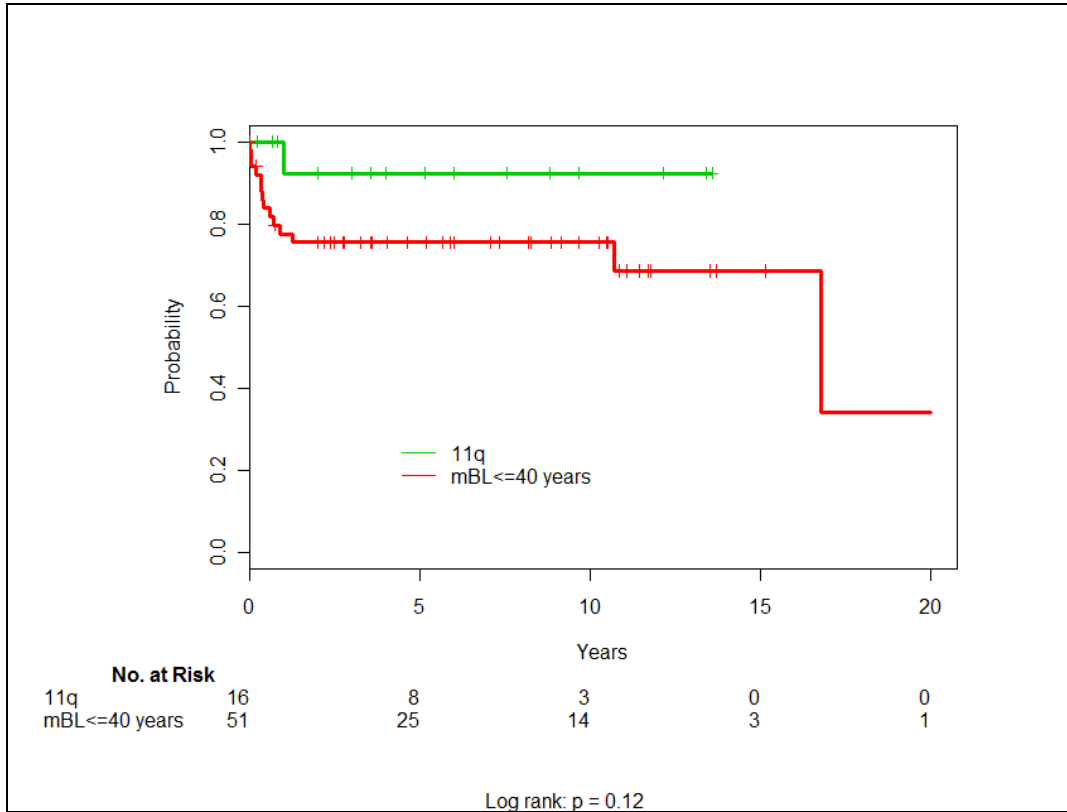
Supplemental Figure 3. Methylation analysis of hsa-mir-34b. Methylation levels of hsa-mir-34b in *MYC*-negative high-grade lymphomas (cohort 2) in comparison with *IG-MYC*-positive molecular BL and cell lines.



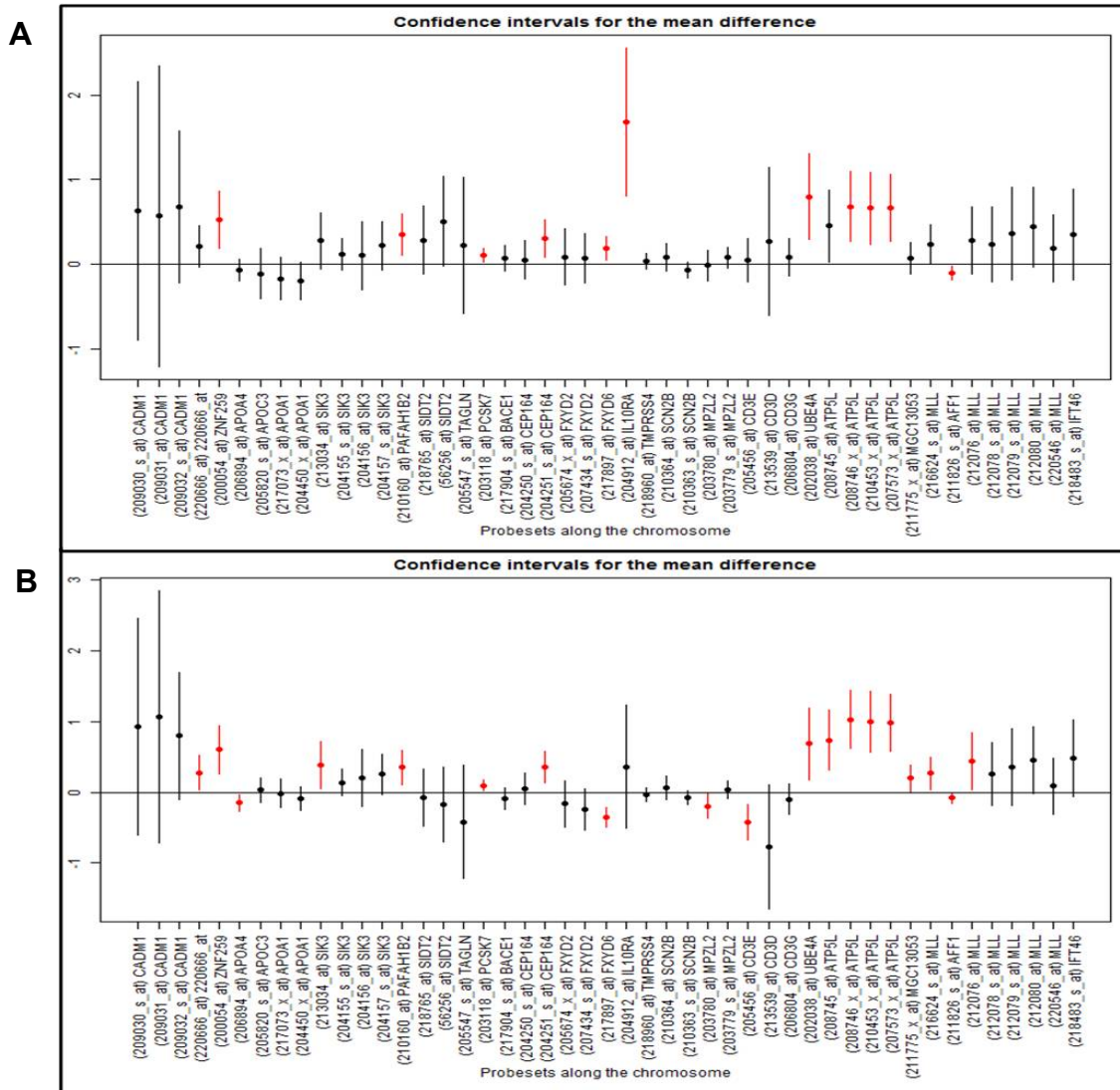
Supplemental Figure 4. 11q alterations in cohort 2 and cohort 3. Diagrams of (A) focal homozygous deletion of 11q24.2-q24.3 of case 9 from the cohort 2 (B) breakpoint region defined as change from gain to loss at chromosome 11. Fragile sites FRAG11G and FRAG11B location region according to Fechter *et al*²⁵ are indicated as green and orange lines, respectively.

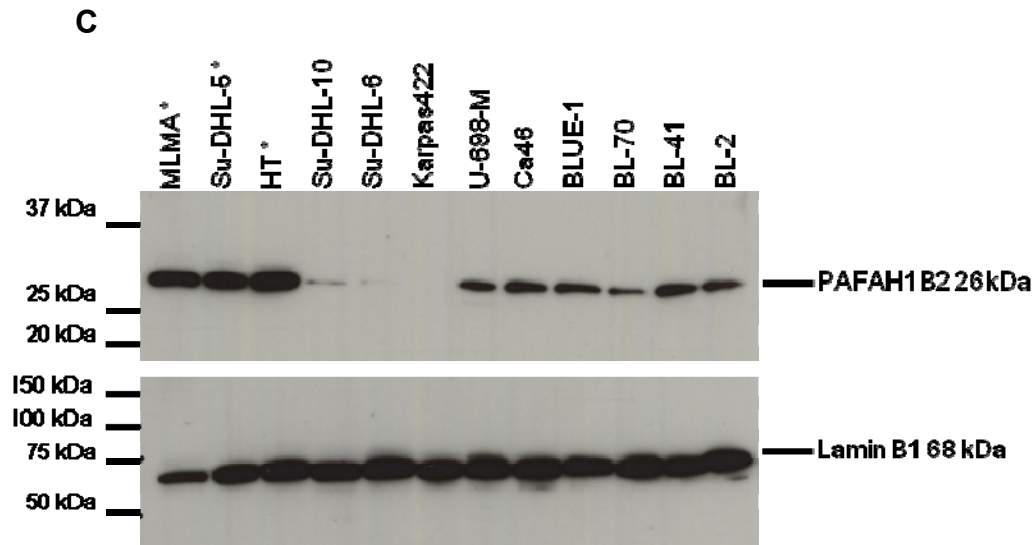


Supplemental Figure 5. Survival analysis in the *MYC*-negative 11q lymphomas. Kaplan-Meier analysis comparing cases with the 11q-gain/loss pattern (cohort 2 and cohort 3, n=16) with *IG-MYC* positive mBL cases (≤ 40 years, n=51).



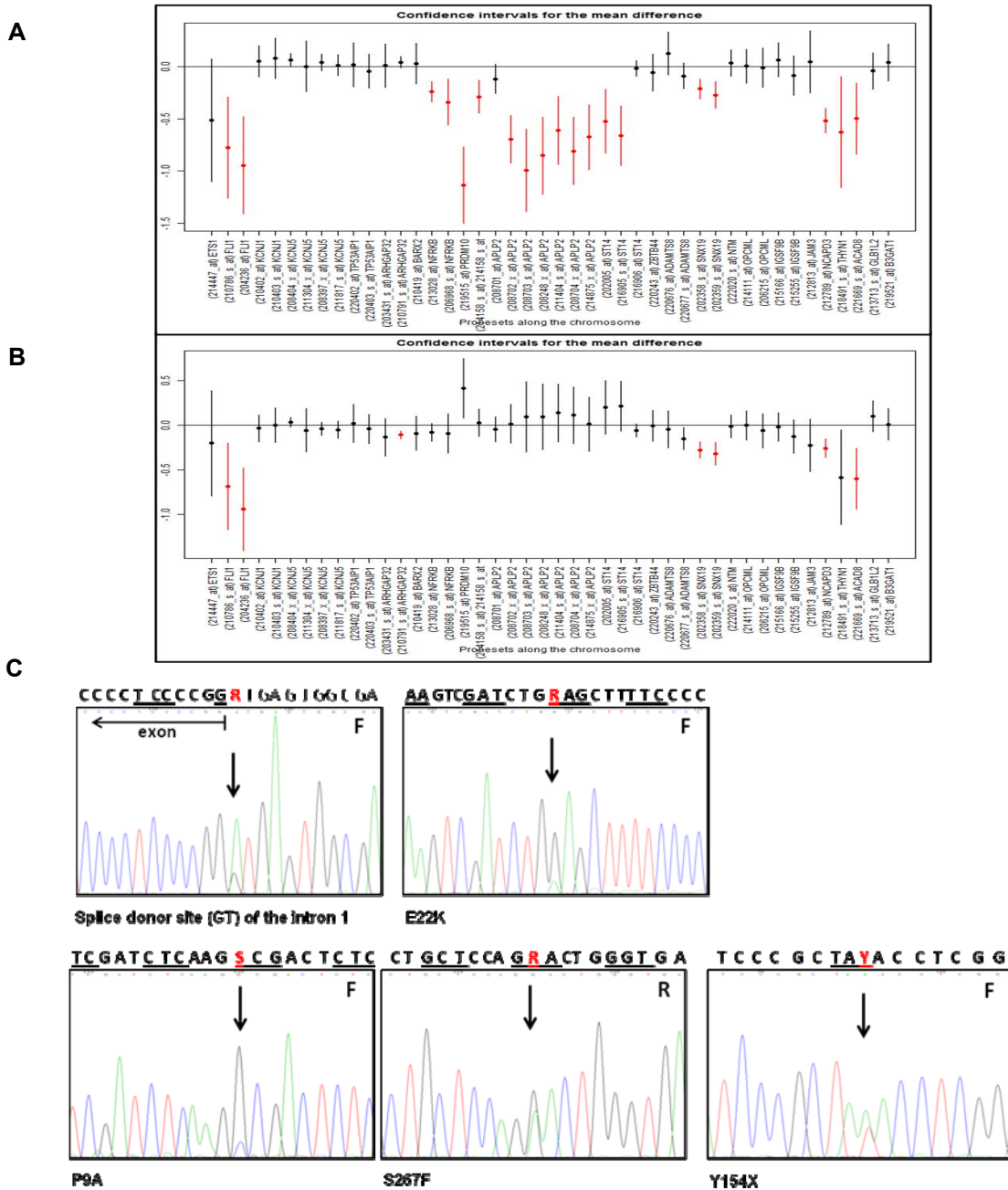
Supplemental Figure 6. Differentially expressed genes located in the minimal region of gain chr11:114530818-117939359 (n=47 probesets). Comparison of GEP of the cases with 11q alterations (cohort 3) (n=6) versus (A) *IG-MYC* mBL (n=46) and (B) DLBCL (n=198). Probesets with FDR < 0.1 are shown in red. Vertical lines indicate univariate 95% confidence intervals for the fold changes between the two compared groups. (C) Western blot showing the protein expression level of the *PFAFH1B2* gene which lie within the minimal region of gain on chromosome 11q, in different cell lines. Asterisks indicate those cell lines with known 11q aberration.



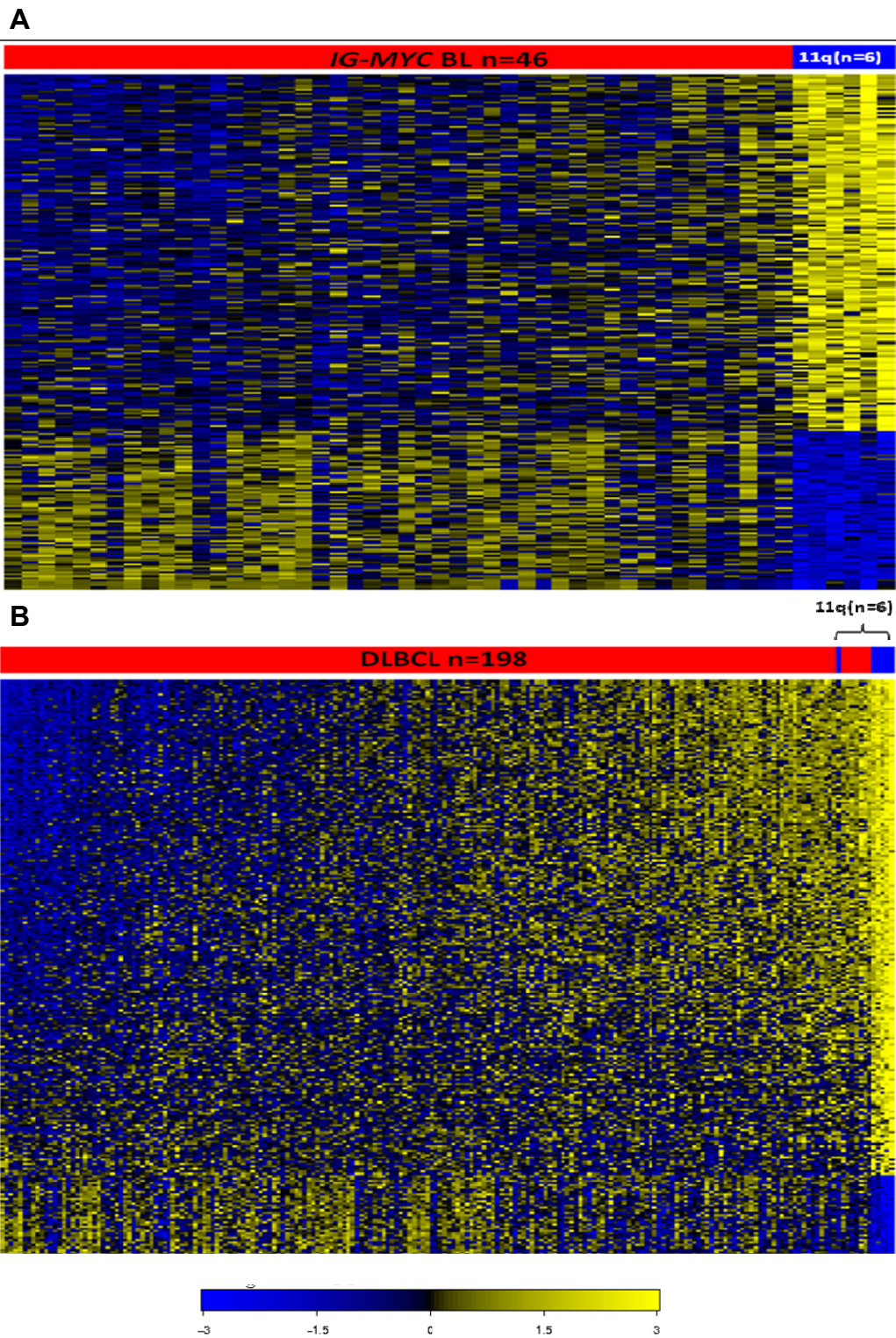


Remark: The MLMA cell line also shows the typical pattern of 11q aberration identified in this paper (see: <http://www.sanger.ac.uk/genetics/CGP/CellLines/>, and data not shown). As it has been described as “hairy cell leukemia” or “hairy cell B-cell lymphoma” (<http://cellbank.nibio.go.jp/legacy/celldata/jcra0146.htm>)³⁰ it has not been used for definition of the minimal regions throughout this paper.

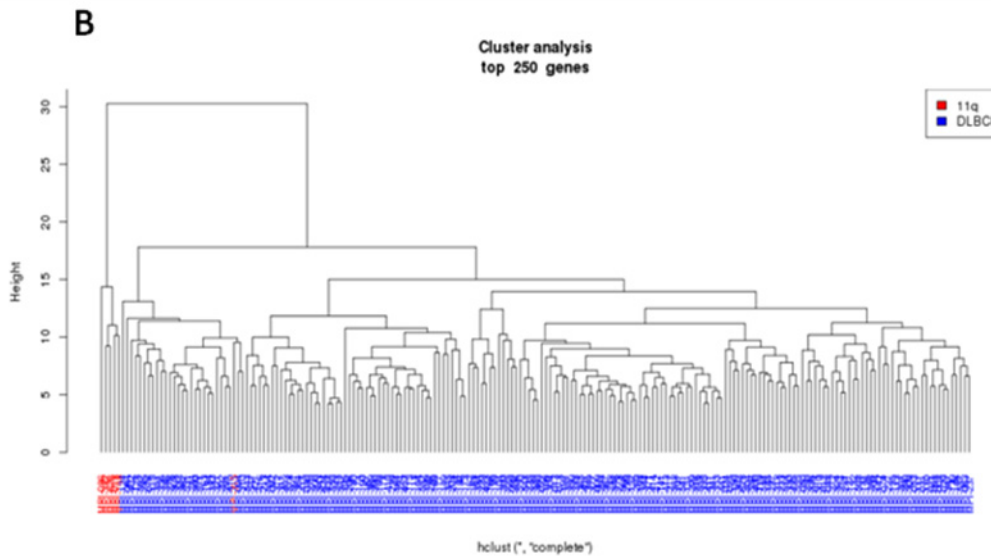
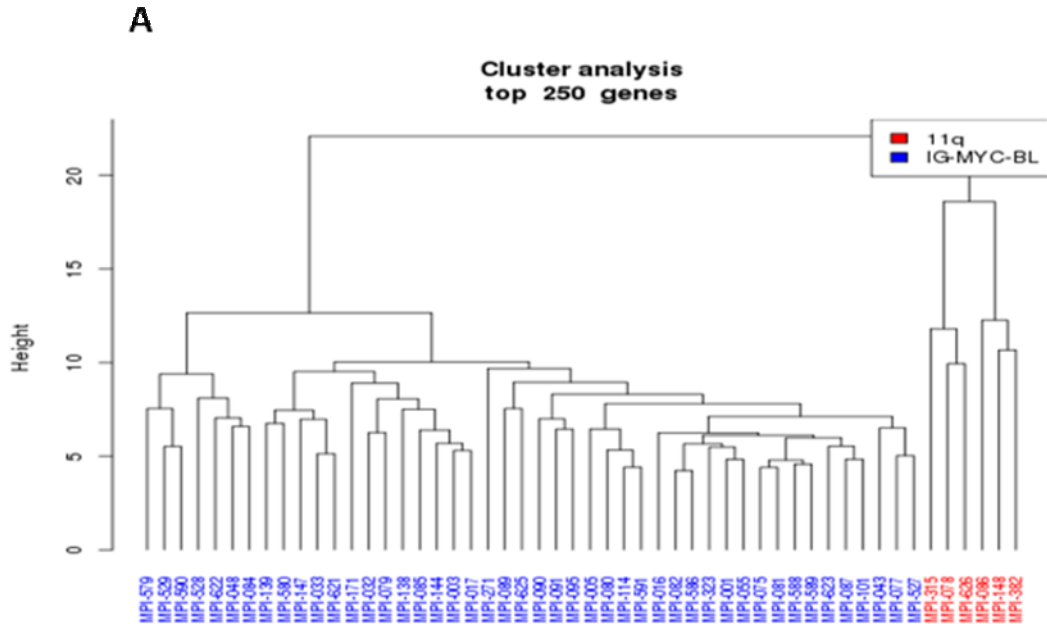
Supplemental Figure 7. Differentially expressed genes located in the minimal region of loss chr11: 126,977,015-134,445,937 (n=44 probesets). Comparison of the GEP of the cases with 11q-gain/loss pattern (cohort 3) (n=6) *versus* (A) *IG-MYC* molecular BL (n=46) and (B) DLBCL (n=198). Probesets with FDR < 0.1 are shown in red. Vertical lines indicate univariate 95% confidence intervals for the fold changes between the two compared groups. (C) Non-synonymous mutations detected on the *ETS1* gene, corresponding to three transitions and two transversions. In total, three mutations were missense, one was located in the splice donor site of the intron 1 and another one was an inactivating mutation (p.Y154X).



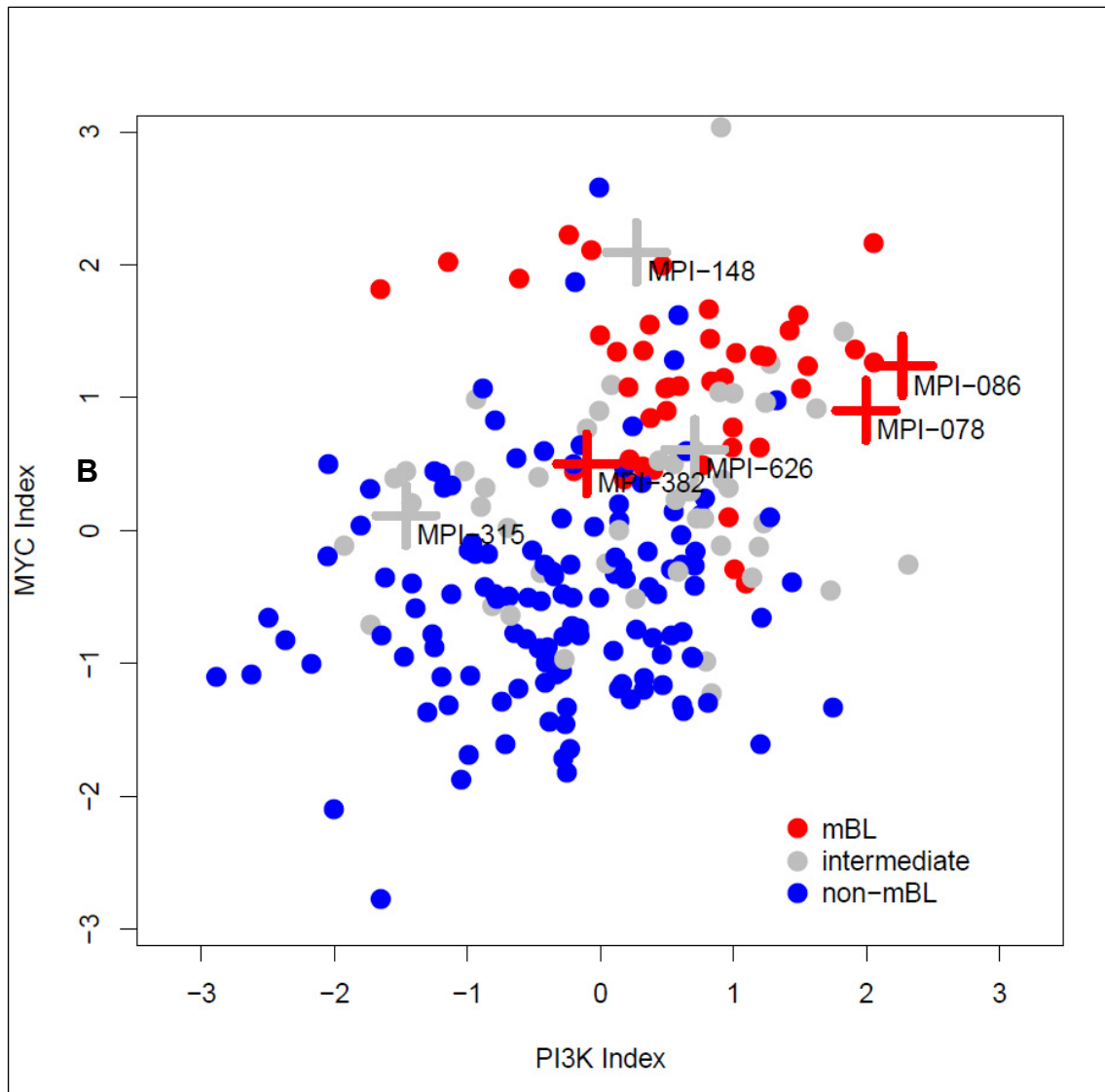
Supplemental Figure 8. GEP analysis of 11q-gain/loss pattern versus *IG-MYC* BL and DLBCL. Heatmap of Top 250 differentially expressed genes (A) *IG-MYC* BL (n=46) versus cohort 3 (n=6) (B) DLBCL (n=198) versus cohort 3 (n=6).



Supplemental Figure 9. Cluster analysis. (A) Clear separation between 11q-gain/loss pattern (red) and *IG-MYC* BL samples (blue) with no group-interference. Distance calculation based on Top 250 differentially expressed genes. (B) Clear separation between 11q-gain/loss pattern (red) and DLBCL samples (blue) with only MPI-315 appearing closer related to the DLBCL. Distance calculation based on Top 250 differentially expressed genes.



Supplemental Figure 10. Scatter Plot of the PI3K pathway activity against MYC activation index in human BL.³¹ Cases were classified as molecular BL (mBL), intermediate, and non-mBL in the original study and shown as red, grey and blue dots respectively. Cases with 11q-gain/loss pattern are represented with a cross.



VI. Supplemental references

1. Pienkowska-Grela B, Rymkiewicz G, Grygalewicz B et al. Partial trisomy 11, dup(11)(q23q13), as a defect characterizing lymphomas with Burkitt pathomorphology without MYC gene rearrangement. *Med Oncol*. 2011;28(4):1589-1595.
2. Rymkiewicz G, Walewski J, Blachnio K et al. MYC negative BL with a partial trisomy 11, dup(11)(q23.3q13.1). Can inverted duplication of CCND1, ATM and MLL genes be a substitute for MYC translocations? *Unpublished*. 2013
3. Hummel M, Bentink S, Berger H et al. A biologic definition of Burkitt's lymphoma from transcriptional and genomic profiling. *N Engl J Med*. 2006;354(23):2419-2430.
4. Bentink S, Wessendorf S, Schwaenen C et al. Pathway activation patterns in diffuse large B-cell lymphomas. *Leukemia*. 2008;22(9):1746-1754.
5. Oschlies I, Salaverria I, Mahn F et al. Pediatric follicular lymphoma--a clinico-pathological study of a population-based series of patients treated within the Non-Hodgkin's Lymphoma--Berlin-Frankfurt-Munster (NHL-BFM) multicenter trials. *Haematologica*. 2010;95(2):253-259.
6. Martin-Guerrero I, Salaverria I, Burkhardt B et al. Recurrent loss of heterozygosity in 1p36 associated with TNFRSF14 mutations in IRF4 translocation negative pediatric follicular lymphomas. *Haematologica*. 2013;98(8):1237-1241.
7. Swerdlow S, Campo E, Harris N et al (Editors). WHO Classification of Tumours of Haematopoietic and Lymphoid Tissues. Lyon, 2008.
8. Nagel I, Akasaka T, Klapper W et al. Identification of the gene encoding cyclin E1 (CCNE1) as a novel IGH translocation partner in t(14;19)(q32;q12) in diffuse large B-cell lymphoma. *Haematologica*. 2009;94(7):1020-1023.
9. Korn JM, Kuruvilla FG, McCarroll SA et al. Integrated genotype calling and association analysis of SNPs, common copy number polymorphisms and rare CNVs. *Nat Genet*. 2008;40(10):1253-1260.
10. Kreuz M, Rosolowski M, Berger H et al. Development and implementation of an analysis tool for array-based comparative genomic hybridization. *Methods Inf Med*. 2007;46(5):608-613.
11. Li H, Handsaker B, Wysoker A et al. The Sequence Alignment/Map format and SAMtools. *Bioinformatics*. 2009;25(16):2078-2079.
12. Jones DT, Jager N, Kool M et al. Dissecting the genomic complexity underlying medulloblastoma. *Nature*. 2012;488(7409):100-105.
13. Richter J, Schlesner M, Hoffmann S et al. Recurrent mutation of the ID3 gene in Burkitt lymphoma identified by integrated genome, exome and transcriptome sequencing. *Nat Genet*. 2012;44(12):1316-1320.
14. Wang K, Li M, Hakonarson H. ANNOVAR: functional annotation of genetic variants from high-throughput sequencing data. *Nucleic Acids Res*. 2010;38(16):e164.
15. Quinlan AR, Hall IM. BEDTools: a flexible suite of utilities for comparing genomic features. *Bioinformatics*. 2010;26(6):841-842.

16. Smyth GK. Linear models and empirical bayes methods for assessing differential expression in microarray experiments. *Stat Appl Genet Mol Biol*. 2004;Article 3.
17. Benjamini Y, Hochberg Y. Controlling the false discovery rate: a practical and powerful approach to multiple testing. *Journal of the Royal Statistical Society, Series B (Methodological)*. 1995;57:289-300.
18. Pollard K, Dudoit S, van der Laan M. Multiple Testing Procedures: R multitest Package and Applications to Genomics. *Bioinformatics and Computational Biology Solutions Using R and Bioconductor*.: Springer; 2005:251-272.
19. Wang X, Terfve C, Rose JC, Markowitz F. HTSanalyzeR: an R/Bioconductor package for integrated network analysis of high-throughput screens. *Bioinformatics*. 2011;27(6):879-880.
20. Leucci E, Cocco M, Onnis A et al. MYC translocation-negative classical Burkitt lymphoma cases: an alternative pathogenetic mechanism involving miRNA deregulation. *J Pathol*. 2008;216(4):440-450.
21. Biggar RJ, Nkrumah FK, Henle W, Levine PH. Very late relapses in patients with Burkitt's lymphoma: clinical and serologic studies. *J Natl Cancer Inst*. 1981;66(3):439-444.
22. Koduru PR, Offit K, Jhanwar SC. Molecular analysis of structural chromosome changes affecting chromosome band 11q23. *Dis Markers*. 1989;7(3):145-152.
23. Mikraki V, Jhanwar SC, Filippa DA, Wollner N, Chaganti RS. Distinct patterns of chromosome abnormalities characterize childhood non-Hodgkin's lymphoma. *Br J Haematol*. 1992;80(1):15-20.
24. Poirel HA, Cairo MS, Heerema NA et al. Specific cytogenetic abnormalities are associated with a significantly inferior outcome in children and adolescents with mature B-cell non-Hodgkin's lymphoma: results of the FAB/LMB 96 international study. *Leukemia*. 2009;23(2):323-331.
25. Fechter A, Buettel I, Kuehnel E, Savelyeva L, Schwab M. Common fragile site FRA11G and rare fragile site FRA11B at 11q23.3 encompass distinct genomic regions. *Genes Chromosomes Cancer*. 2007;46(1):98-106.
26. Krug U, Ganser A, Koeffler HP. Tumor suppressor genes in normal and malignant hematopoiesis. *Oncogene*. 2002;21(21):3475-3495.
27. Mackereth CD, Scharpf M, Gentile LN et al. Diversity in structure and function of the Ets family PNT domains. *J Mol Biol*. 2004;342(4):1249-1264.
28. Oricchio E, Nanjangud G, Wolfe AL et al. The Eph-receptor A7 is a soluble tumor suppressor for follicular lymphoma. *Cell*. 2011;147(3):554-564.
29. Pasqualucci L, Compagno M, Houldsworth J et al. Inactivation of the PRDM1/BLIMP1 gene in diffuse large B cell lymphoma. *J Exp Med*. 2006;203(2):311-317.
30. Saito Y, Miyagawa Y, Onda K et al. B-cell-activating factor inhibits CD20-mediated and B-cell receptor-mediated apoptosis in human B cells. *Immunology*. 2008;125(4):570-590.
31. Sander S, Calado DP, Srinivasan L et al. Synergy between PI3K signaling and MYC in Burkitt lymphomagenesis. *Cancer Cell*. 2012;22(2):167-179.